EVALUATION OF TWO DIMENSIONAL HF ADAPTIVE ANTENNA ARRAYS

R. L. St. Germain, et al

Raytheon Company

Prepared for:

Defense Advanced Research Projects Agency
Rome Air Development Center

October 1974

UNCLASSIFIED

SECURITY CLASSIFICATION OF THIS PAGE (When Data Entered)

REPORT DOCUMENTATION PAGE	READ INSTRUCTIONS BEFORE COMPLETING FORM
1. REPORT NUMBER: RADC-TR-74-281	2. GOVT ACCESSION NO.
3. RECIPIENT'S CATALOG NUMBER: AD/A-001088	
4. TITLE (and Subtitle): Evaluation of Two Dimensional HF Adaptive Antenna Arrays	5. TYPE OF REPORT & PERIOD COVERED: Final Technical Report
6. PERFORMING ORG. REPORT NUMBER: ER74-4272	
7. AUTHOR(s): R. L. St. Germain, H. R. Alexander, Dr. G. D. Thome	8. CONTRACT OR GRANT NUMBER(s): F30602-73-C-0265
9. PERFORMING ORGANIZATION NAME AND ADDRESS: Raytheon Company, 528 Boston Post Rd, Sudbury MA 01776	10. PROGRAM ELEMENT, PROJECT, TASK AREA & WORK UNIT NUMBERS: 62301E, 23850201
11. CONTROLLING OFFICE NAME AND ADDRESS: Defense Advanced Research Projects Agency, 1400 Wilson Blvd, Arlington VA 22209	12. REPORT DATE: October 1974 13. NUMBER OF PAGES: 66
14. MONITORING AGENCY NAME & ADDRESS(if different from Controlling Office): Rome Air Development Center (OCSE), ATTN: Leonard Strauss, Griffiss AFB NY 13441	15. SECURITY CLASS. (of this report): UNCLASSIFIED 15a. DECLASSIFICATION/DOWNGRADING SCHEDULE: N/A

16. DISTRIBUTION STATEMENT (of this Report)

Approved for public release. Distribution unlimited.

17. DISTRIBUTION STATEMENT (of the abstract entered in Block 20, if different from Report)

Approved for public release. Distribution unlimited.

18. SUPPLEMENTARY NOTES

None

19. KEY WORDS (Continue on reverse side if necessary and identify by block number)

HF Antenna Arrays
Adaptive Antenna Processors
Two Dimensional Arrays
Digital Beamformers

20. ABSTRACT (Continue on reverse side if necessary and identify by block number)

The DARPA HF Adaptive Array Program has been a one year, three component effort (University of Colorado, Stanford Research Institute, and Raytheon) to determine the applicability of known adaptive antenna processing techniques to HF systems. This report is the final report on the Raytheon portion of this program. The Raytheon effort emphasized the evaluation two-dimensional adaptive arrays in the real HF environment. The primary task was to modify an existing HF phased array facility in

DD FORM 1 JAN 73 1473 EDITION OF 1 NOV 65 IS OBSOLETE

UNCLASSIFIED

SECURITY CLASSIFICATION OF THIS PAGE (When Data Entered)

Hudson, Colorado so that data could be collected on a large two-dimensional array in a format suitable for use by Raytheon and by others for adaptive processing. The principal modifications included the construction of a 32 element cross array of vertical monopoles and the addition of quadrature outputs to the existing 32-channel receiver and data acquisition system. Additional Raytheon tasks included the development of software (for controlling the data collection system, for processing and displaying the field data, for producing simulated field tapes for specific array geometries and model environments), data collection under a variety of conditions, and analysis (numerical simulations to guide the design of the antenna array and data reduction to evaluate the performance improvement obtained through adaptive processing).

The principal result of this work is the verification that the HF environment will in fact permit most of the performance improvement anticipated from idealized numerical simulations of adaptive processing applied to large two-dimensional arrays. Noise floor reductions of order 30 dB (compared to conventional processing) were realized over most of the radio sky under conditions in which a single strong interferer was present (10 dB element signal to noise ratio). Viewed as a technique for producing improved two-dimensional maps of the radio environment (e.g., radio location or noise survey applications) rather than for improving signal to noise ratio, the maps produced by adaptive beamforming exhibit superior angular definition and apparent freedom from sidelobe responses. That is, the adaptive processor is effective in deconvolving the antenna pattern from the measurements.

The HF environment is found to change rapidly enough so that if a one second block of data is processed with adaptive weights computed for the preceding one second data block, approximately 10 dB of the noise floor improvement attainable by using optimum weights is lost. It appears that the direct matrix inversion method for implementing adaptive processing will in practice require a new inversion for each data block but it has not yet been determined how long these data blocks can be made without incurring an unacceptable signal to noise ratio penalty.

It was found that the output of the adaptive processor was typically 20 dB less than that of the conventional processor when both were pointed in the source direction, an unexpected effect (ideally they would be equal) attributed to the departure of the wavefront of the incident signal from an ideal plane wave. This departure is believed due to ionospheric multipath but terrain scattering and/or residual calibration errors in the receiving system cannot be ruled out.

The result of the array geometry study is to suggest low-redundancy sparse arrays as promising candidates for adaptive antenna applications in which both angular resolution and signal to noise ratio are considerations.

It is recommended that the processing of the data base already on tape be completed so as to explore the impact of variable data block length on signal to noise ratio, to explore the consequences of simultaneous adaptivity in azimuth, elevation, and frequency, and to explore the performance of the adaptive processor in complex interference environments.

EVALUATION OF TWO DIMENSIONAL HF ADAPTIVE ANTENNA ARRAYS

R. L. St. Germain
H. R. Alexander
Dr. G. D. Thome

Contractor: Raytheon Company
Contract Number: F30602-73-C-0265
Effective Date of Contract: 2 April 1973
Contract Expiration Date: 30 March 1974
Amount of Contract: $134,357.00
Program Code Number: 4E20

Period Covered - 2 Apr 73 - 19 Aug 74

Principal Investigator: Dr. G. D. Thome
Phone: 617 443-9521, Ext. 2103

Project Engineer: Leonard Strauss
Phone: 315 330-3055

This research was supported by the Defense Advanced Research Projects Agency of the Department of Defense and was monitored by Leonard Strauss, RADC (OCSE), GAFB NY 13441 under Contract F30602-73-C-0265, Job Order No. 23850201.

This report has been reviewed by the RADC Information Office (OI), and is releasable to the National Technical Information Service (NTIS).

This technical report has been reviewed and is approved.

Leonard Strauss
RADC Project Engineer

ABSTRACT

The DARPA HF Adaptive Array Program has been a one year, three component effort (University of Colorado, Stanford Research Institute, and Raytheon) to determine the applicability of known adaptive antenna processing techniques to HF systems. This report is the final report on the Raytheon portion of this program. The Raytheon effort emphasized the evaluation two-dimensional adaptive arrays in the real HF environment. The primary task was to modify an existing HF phased array facility in Hudson, Colorado so that data could be collected on a large two-dimensional array in a format suitable for use by Raytheon and by others for adaptive processing. The principal modifications included the construction of a 32 element cross array of vertical monopoles and the addition of quadrature outputs to the existing 32-channel receiver and data acquisition system. Additional Raytheon tasks included the development of software (for controlling the data collection system, for processing and displaying the field data, for producing simulated field tapes for specific array geometries and model environments), data collection under a variety of conditions, and analysis (numerical simulations to guide the design of the antenna array and data reduction to evaluate the performance improvement obtained through adaptive processing).

The principal result of this work is the verification that the HF environment will in fact permit most of the performance improvement anticipated from idealized numerical simulations of adaptive processing applied to large two-dimensional arrays. Noise floor reductions of order 30 dB (compared to conventional processing) were realized over most of the radio sky under conditions in which a single strong interferer was present (10 dB element signal to noise ratio). Viewed as a technique for producing improved two-dimensional maps of the radio environment (e.g., radio location or noise

survey applications) rather than for improving signal to noise ratio, the maps produced by adaptive beamforming exhibit superior angular definition and apparent freedom from sidelobe responses. That is, the adaptive processor is effective in deconvolving the antenna pattern from the measurements.

The HF environment is found to change rapidly enough so that if a one second block of data is processed with adaptive weights computed for the preceding one second data block, approximately 10 dB of the noise floor improvement attainable by using optimum weights is lost. It appears that the direct matrix inversion method for implementing adaptive processing will in practice require a new inversion for each data block but it has not yet been determined how long these data blocks can be made without incurring an unacceptable signal to noise ratio penalty.

It was found that the output of the adaptive processor was typically 20 dB less than that of the conventional processor when both were pointed in the source direction, an unexpected effect (ideally they would be equal) attributed to the departure of the wavefront of the incident signal from an ideal plane wave. This departure is believed due to ionospheric multipath but terrain scattering and/or residual calibration errors in the receiving system cannot be ruled out.

The result of the array geometry study is to suggest low-redundancy sparse arrays as promising candidates for adaptive antenna applications in which both angular resolution and signal to noise ratio are considerations.

It is recommended that the processing of the data base already on tape be completed so as to explore the impact of variable data block length on signal to noise ratio, to explore the consequences of simultaneous adaptivity in azimuth, elevation, and frequency, and to explore the performance of the adaptive processor in complex interference environments.

TABLE OF CONTENTS

1.0 INTRODUCTION

1.1 OBJECTIVES

The DARPA HF Adaptive Antenna program has been a three component program involving the Stanford Research Institute (SRI), the University of Colorado (U of C) and Raytheon. The overall objective of the program has been to determine the applicability of known adaptive processing techniques to HF antenna arrays. The motivation for the program has come from the impressive improvements in array performance obtained by applying adaptive processing to sonar, seismic, and microwave systems. The need for an HF program arises because the benefits derived from adaptive processing depend strongly upon the characteristics of the noise and interference environment (e.g., temporal and spatial stability): consequently, performance improvements obtained at microwave frequencies are not necessarily good indicators of what can be expected at HF frequencies. To obtain the necessary data base at HF and to test the applicability of adaptive algorithms developed with other environments in mind, the DARPA program was structured in the following way: SRI modified the receiver system for the WARF antenna so as to provide data for adaptive processing from a large one-dimensional array, Raytheon made modifications to the DARPA HF phased array facility at Hudson, Colorado so as to provide data for adaptive processing on a large two-dimensional array, and U of C provided algorithm research and processing expertise. An interim report on the Raytheon component of the program was published in March 1974: (Reference 1) the material presented here is the final report on this effort.

1.2 SCOPE OF THE EFFORT

The primary task (70% of the effort) was to modify the Hudson phased array facility so that data could be collected on a large two-dimensional array in a format suitable for use by ourselves and by others for adaptive processing. Two principal modifications were required: First, the receiver system was modified to provide simultaneous quadrature samples for each element of a 32 element array. The original receiver system consisted of a bank of 32 receiver modules, each with a single real output and a single sample and hold circuit. Quadrature outputs were provided by fabricating an identical set of 32 receiver modules, shifting the phase of the local oscillator (HFO) for this set by 90^{o} from the first set, and using one receiver module from each set for each antenna. This provided the complex samples required in adaptive processing. The second facility modification was to build a cross array of 32 vertical monopole elements with base amplifiers. The original facility array was a circular array with horizontal crossed dipole elements intended for diagnosing the overhead ionosphere. This array was not suitable for studying the low elevation angle signals of primary interest in adaptive antenna applications.

The second major task (15% of the effort) was the development of software for three purposes:

1. field software for controlling the data acquisition system and for providing on-site diagnostic information.
2. analysis software for processing and displaying the field data using conventional and adaptive two-dimensional beamforming algorithms.
3. simulation software to generate data tapes for model signal environments and for model array configurations to use in

testing the analysis software and for studying the effects of array configuration on processor performance.

The third task was data collection (5% of the effort) which involved preparing and manning the Hudson phased array site for three days of data taking (two days in November, 1973 and one day in January, 1974). Data were collected with SRI providing cw transmissions at several different power levels and frequencies. Data were also collected in a variety of uncooperative interference environments such as the amateur radio bands and the international broadcast bands.

The fourth task was data analysis (10% of the effort). The analysis involved the reduction of selected portions of the data base with conventional and adaptive processing and the evaluation of the results to determine such things as the stability of the environment and the noise floor reduction achieved. This task also included considering the effect of array geometry on adaptive processor performance.

1.3 ORGANIZATION OF THE REPORT

This report is written for the reader who is familiar with HF systems and the problems they encounter when operated in the real world: a background in adaptive processing is not assumed. The presentation begins (Section 2.0) with a brief statement of the theory and the processing algorithms on which our work has been based. A series of computer simulations is then presented (Section 3.0) to illustrate the operation of adaptive processors under ideal conditions, to document the research which has been done on the properties of low-redundancy sparse arrays when used with adaptive beamformers, and to provide the basis for comparing the theory with the field measurements. Section 4.0 includes a description of the two-dimensional

antenna array used in this program and a discussion of the data base collected. An analysis of selected portions of this data base is given in Section 5.0. The results of the Raytheon component of the program are summarized in Section 6.0.

2.0 THEORETICAL BACKGROUND

The purpose of this section is to give a brief statement of the mathematics which has been used in the software codes for conventional and adaptive processing. The mathematics is particularly simple and compact in matrix notation and this form of the equations will be used for convenience. This section also includes a discussion of the effect of receiver errors on adaptive beamformers, in preparation for the analysis of experimental data to be presented in Section 5.0.

2.1 BEAMFORMER OPERATION

Beamforming is the process of estimating the signal power arriving from a given direction and amounts to summing the signals from each array element after applying an appropriate set of complex weights. The process is illustrated schematically in Figure 1 and is the same operation whether conventional or adaptive processing has been used to determine the weights. It is assumed that the array has M elements and that the receiver output from each element is sampled simultaneously to give a set of M complex samples, $x_1, x_2, \ldots\ldots x_M$. These samples are weighted with a set of complex weights to form a new data set ($x_1 w_1, x_2 w_2, \ldots\ldots x_M w_M$) and this new data set is summed to give a complex number, y, as the beamformer output. If the set of weights is written as a column vector W and the set of data samples as a column vector X, then the beamformer operation can be written in matrix notation as

$$y = W^* X \qquad (1)$$

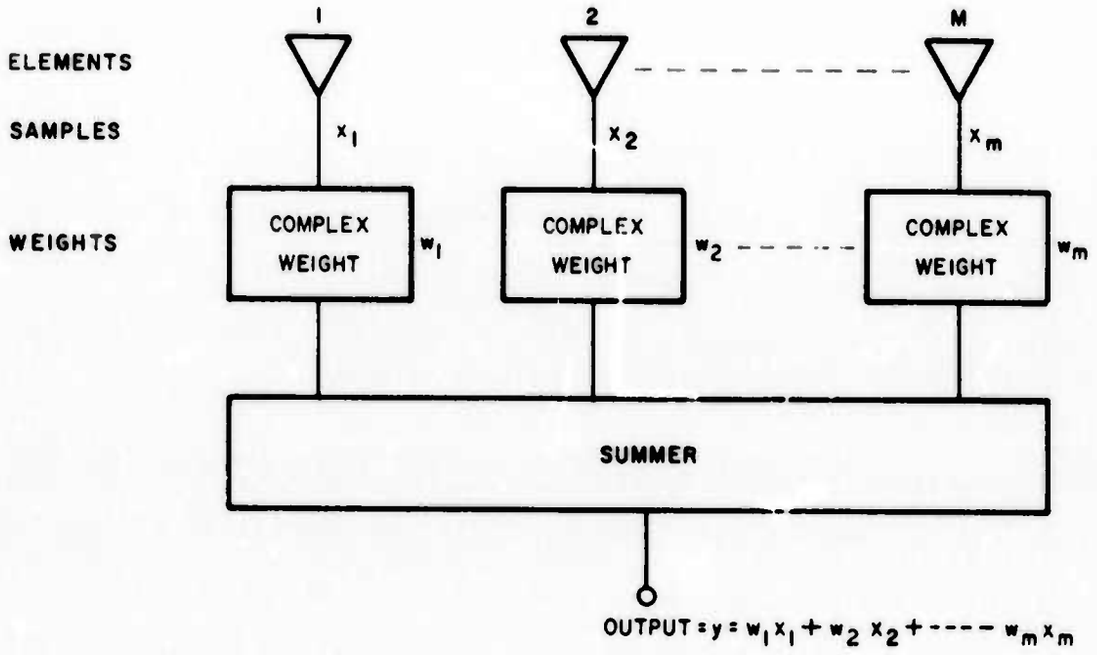

Figure 1. Beamforming Network (Conventional or Adaptive)

where W^* is the conjugate transpose of W (i. e., a row vector with elements equal to the complex conjugate of the elements in W). This gives the beamformer output for one time sample of the array outputs. In this report this process is always repeated for 64 time samples of the array, the power output computed for each sample, and the results averaged to give the average power arriving from the direction of interest.

2.2 CONVENTIONAL WEIGHTS

In conventional beamforming, the computation of the weights to form a beam in a given direction begins by computing the signal expected at each element of the array for a plane wave of unit amplitude arriving from the desired direction. This set of complex numbers $(v_1, v_2 \ldots . v_M)$ is written as a column vector V and this is called the steering vector for that direction. In conventional beamforming the weight vector is set equal to the steering vector and consequently

$$W^* = V^* \tag{2}$$

for use in the beamformer of equation (1). A constant of proportionality could be added to the right side of this equation without affecting the antenna pattern or the SNR but we elect to choose this constant to be unity in order to keep the expression as simple as possible. With this choice, the output of the conventional beamformer will be M units when steered to look in the direction of a plane wave of unit amplitude at each element.

If the background noise environment is omni-directional (a "white" angular noise spectrum) the conventional weights are known to give the maximum signal to noise ratio (SNR) out of the beamformer. In practice this condition is seldom if ever met and in this case (a "colored" angular noise spectrum) the optimum weights must be adapted to match the environment if

maximum SNR is to be obtained.

2.3 ADAPTIVE WEIGHTS

The first step in computing the adaptive weights is to compute the average covariance matrix for the array. This covariance matrix, F, is an M by M matrix made up of the average covariance between all pairs of elements (e.g., $f_{1,7}$ is the covariance between the first element and the seventh). This matrix characterizes the environment over the period of interest. The conjugate transpose of the weight vector is then given (Griffiths, Reference 2) by

$$W^* = b\, V^*\, F^{-1} \tag{3}$$

where b is a constant which normalizes the set of weights in a convenient manner, V^* is the conjugate transpose of the steering vector, and F^{-1} is the inverse of the covariance matrix. It is convenient to choose the constant b so that the output of the adaptive beamformer will equal the output of the conventional beamformer when both are steered in the direction of a plane wave of unit amplitude at each element. The appropriate constant (Capon, Reference 3) is

$$b = M/V^*\, F^{-1} V \tag{4}$$

Equations (1), (3), and (4) constitute the adaptive beamformer as implemented in this report.

2.4 RECEIVER ERRORS

In any practical beamformer the received data samples are somewhat in error because the M data channels have residual gain and phase shift differences between chanrels. The effect of these errors has been discussed extensively for conventional beamforming. The effect of errors in the data samples or in the weighting function of adaptive processors has also received

some attention. McDonough (Reference 4) has provided some insight into effects of such errors, and relates his results to those of other authors. He points out that in conventional beamforming, the principal effect of errors is in the "sidelobe" region of an antenna pattern. With adaptive or optimum processors, a degrading effect on the resolution properties near a discrete source is noted.

As McDonough notes, the effect of errors in the receiving channels will vary depending on how the errors appear in the adaptive beamformer. Thus, it is desirable to consider the effect of errors in the manner in which they are most likely introduced in the system being evaluated.

For the experimental data discussed in this report, the environment is essentially a discrete interfering source and isotropic noise. With channel to channel gain and phase unbalance, the residual errors cause a modification of the observed covariance matrix relative to the true covariance matrix with no errors. The perturbed covariance matrix is the one used to form the adaptive weights. The response of the processor will be different from the response with no errors. The effect of these errors on the adaptive processor is analyzed below: simulations are presented to check the analysis for the representative case of a discrete source in isotropic noise.

2.4.1 Error Analysis

The samples from the environment in the absence of errors consist of a noise power of N watts at each element (uncorrelated from element to element) and a plane wave signal of S watts at each element. The covariance matrix without errors is

$$\Gamma = NI + SVV^* \qquad (5)$$

where I is the unit diagonal matrix, and V is the steering or signal vector for the discrete source, corresponding to the direction of incidence of the plane wave. The principal effect of channel to channel errors is to produce a corrupted signal vector, V_e, whose elements are nominally those of V, but with small random gain and phase changes, e_i,

$$e_i = (1 \pm E/2)\, e^{\pm E/2} \tag{6}$$

where E is a small number reflecting the error in amplitude or in phase. The present analysis and simulation assumes a pseudorandom binary error model with independent phase and amplitude errors. It would be straightforward to extend the model to Gaussian errors with different magnitudes of amplitude and phase as given by McDonough (Reference 4). The present analysis continues by applying this error to the discrete source. Further analysis and simulation have shown that the effect of corruption of isotropic noise by these errors is negligible in comparison to that of the discrete source, when the source power S is equal to or greater than the noise power, N.

The observed covariance matrix which contains the effect of these errors is

$$F_e = NI + SV_e V_e^* \tag{7}$$

When the adaptive beamformer is steered to the direction of the interference, the reciprocal of the output power is

$$P_v^{-1} = MN\left[\frac{1 + (S/N)\, V_e^* V_e - (S/MN)\, \left|V_e^* V\right|^2}{1 + (S/N)\, V_e^* V_e}\right] \tag{8}$$

This expression results in an output power of M^2S watts due to the plane wave

input where E = 0. Next it is noted that when

$$(S/N)\ V_e^*\ V_e - (S/MN)\ \left|V_e^*\ V\right|^2 >> 1 \qquad (9)$$

the expression (8) for the output power P_v is independent of the input signal power S. This means there is a "saturation" effect in the output of an adaptive beamformer when the conventional output SNR, equal to SM/N, is large enough.

To evaluate the criterion for saturation, the pseudorandom error model is used to compute the values of $V_e^*\ V_e$ and $\left|V_e^*\ V\right|^2$. In estimating these quantities, the approximation will provide representative values for P_v and the criterion for saturation. Using the values for $V_e^*\ V_e \sim M\,(1 + E^2/4)$ and $\left|V_e^*\ V\right|^2 \sim M^2(1 - E^2/4)$, (9) becomes

$$E^2/2 >> \frac{1}{(SM/N)} \qquad (10)$$

and (8) becomes

$$P_v \sim \frac{(MN)}{(E^2)/2} \qquad (11)$$

Thus the criterion for saturation equation (10), is that the error magnitudes must be greater than the reciprocal square root of the conventional output signal to noise power ratio. When this criterion is met, the output power, (11) is a constant regardless of any increase in signal power S.

This analysis can be extended to consider look directions away from the interfering source. In those cases, the output power is not significantly affected as long as the error is small compared with unity. Thus the adaptive beamformer is less sensitive to channel-to-channel errors than the conventional beamformer in the "sidelobe" regions.

2.4.2 Simulation

Simulations were performed using a pseudorandom error code, one for magnitude and another for phase, with a 32 element linear array. Figure 2 shows that for a fixed element SNR, the amount by which the beamformer underestimates the signal level is small for small receiver errors, increases slowly with increasing receiver error at first and then a break-point is reached after which the underestimate increases much more rapidly with receiver error. As the error increases, the break-point is reached sooner for high element SNR than for low, and consequently an adaptive system with a given set of receiver errors will give better estimates of the signal power for weak signals than for strong. Once the break-point has been passed, the beamformer output saturates, in that further increases in element SNR produce no further increase in the output. For example, for an RMS gain error of 10 percent, a 10 dB increase in element SNR from 20 dB to 30 dB results in an additional 10 dB underestimate of the signal level, just compensating for the increase in element SNR and causing the output to remain constant.

It has been assumed in this discussion that the errors are caused by receiver gain and phase unbalance, causing an incident plane wave to look irregular to the processor. Alternately, the errors can be thought of as being introduced by irregularity in the ionosphere, by irregularity in the ground from element to element, or by irregularity caused by scattering from local structures. Whatever the cause, the adaptive processor will underestimate the signal power if the incident wave front does not appear plane to the processor: the curves of Figure 2 allow one to estimate how serious this effect will be.

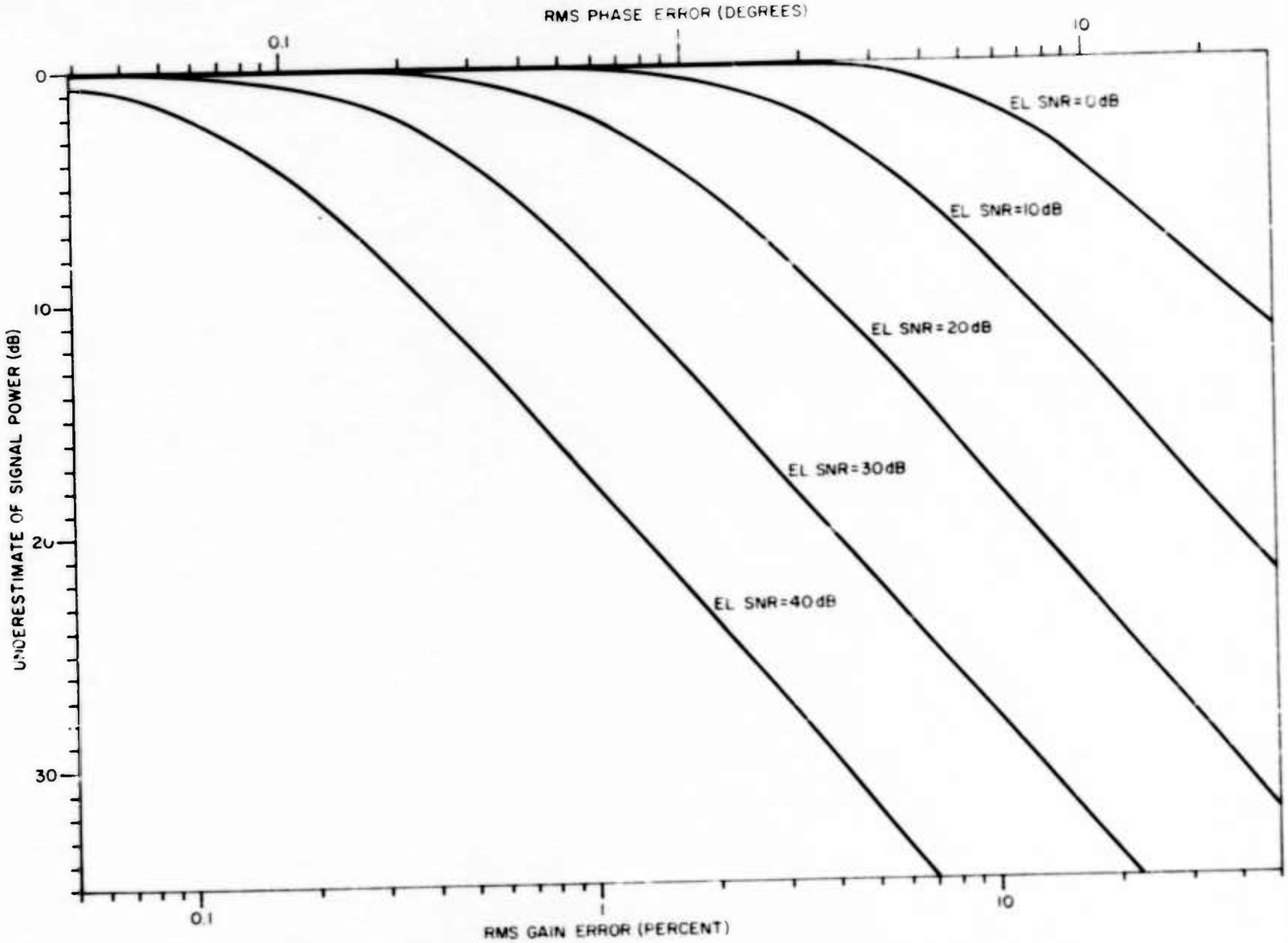

Figure 2. The Relationship between Receiver Errors, Element SNR, and the Amount by which an Adaptive Beamformer will Underestimate the Incident Signal Level (these curves for a 32 element array).

3.0 SIMULATION RESULTS

The algorithms discussed in Section 2.0 for processing two-dimensional array data conventionally and adaptively were implemented in software, along with graphical routines for displaying the results. This software package was written to accept data tapes from the field and has been used to reduce the field data discussed in Section 5.0. A separate software package was also written to generate simulated data tapes for model signal environments and model array geomctries. That is, the intensity, azimuth, elevation, and Doppler shift of a finite number of point sources could be specified along with the intensity of an isotropic background noise level and the number and placement of antenna elements in a one- or two-dimensional array. The simulated data tape contained the time sampled outputs from each element of the array which would be expected under these idealized conditions. These data tapes could then be processed as though they were field tapes. The simulations were used, 1) to verify and debug the processing software (by simulating special cases in which the correct processor output was known), 2) to study the effect of array geometry on processor performance (to decide how to make the best use of the 32 elements available for the collection of field data) and 3), to provide test cases with which to judge whether or not the properties of adaptive processors as predicted from idealized models were realized in practice with real field data. A series of test cases under idealized conditions are given below (Section 3.1) to illustrate the properties expected of adaptive processors. The results of our array geometry study are given in Section 3.2.

3.1 PROPERTIES OF IDEAL ADAPTIVE PROCESSORS

3.1.1 Adaptive Array Antenna Patterns

This section illustrates the interference rejection principle of adaptive beamformers by examining the way in which the antenna pattern changes from one look direction to the next. Stated briefly, an adaptive beamformer affects an improvement is SNR (as compared to a conventional beamformer) by adaptively tailoring the antenna array weights (both in amplitude and phase) in order to set nulls in the corresponding array pattern in the direction of discrete interferers A suitable array gain is simultaneously maintained in the desired look direction so that SNR is maximized.

Consider the seven element linear array shown in Figure 3. The elements are isotropic and spaced by half a wavelength. The simulated signal environment consists of three discrete sources situated at -40, 12, and 30 degrees off boresight with relative strengths of -20, 0, and 0 dB, respectively. The strength of the omni-directional noise is -30 dB (all signal strengths measured at an individual element before any array or processing gain). Working against this environment, the adaptive weights have been computed for look directions of -4 and -40 degrees: the magnitudes of the complex weights for these two look directions are shown as a function of element number at the top of Figure 4. The corresponding patterns of the array for these two look directions are shown at the bottom of this figure. By the "pattern" for a given look direction we mean a plot of the power output of the beamformer (with the adaptive weights for that look direction set in and held fixed) versus the angle to a point source of unit strength. From patterns such as these the following observations can be drawn:

1. The array pattern nulls track the directions of the discrete

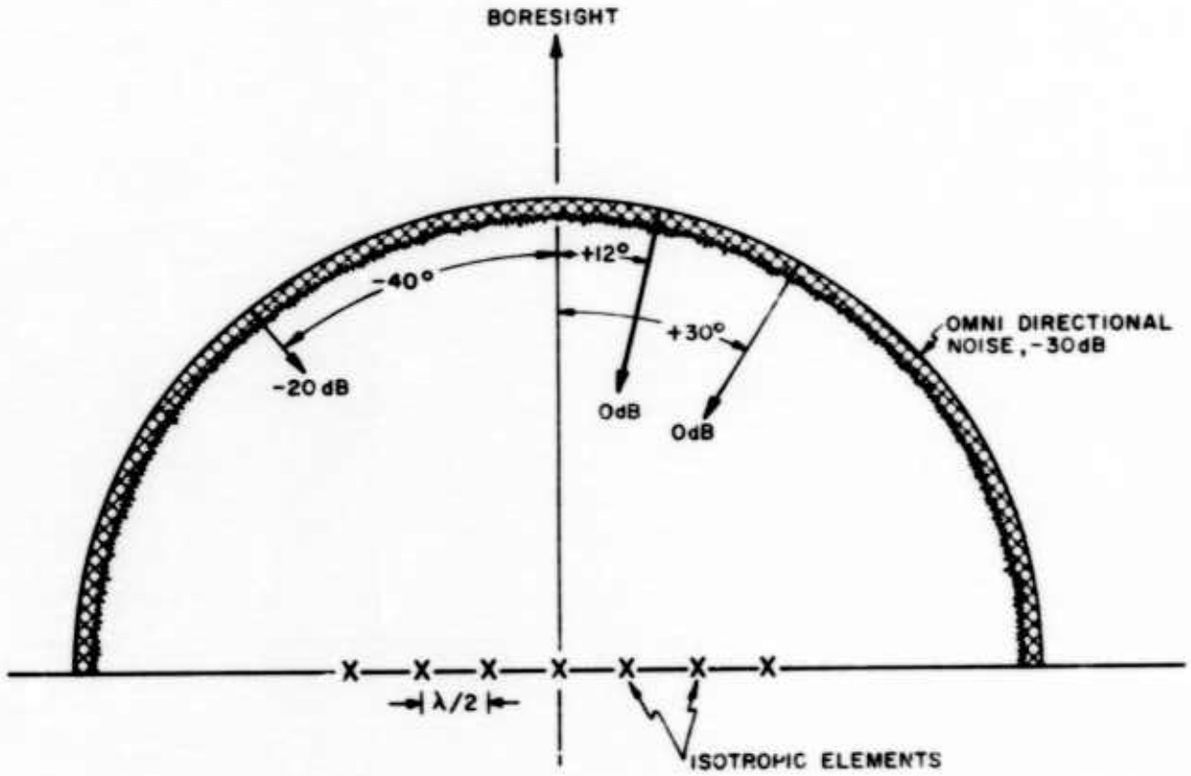

Figure 3. Model Environment Used for Simulations and a Seven Element, Uniformly Spaced Array of Isotropic Radiators

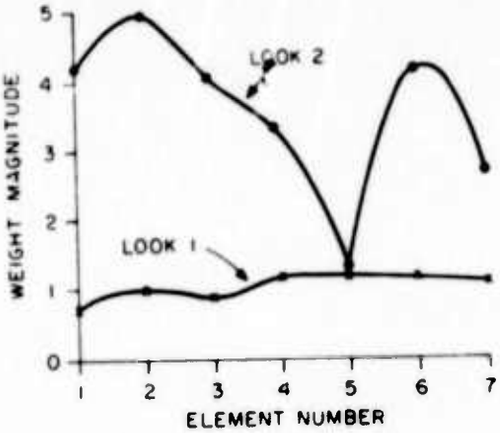

(a)

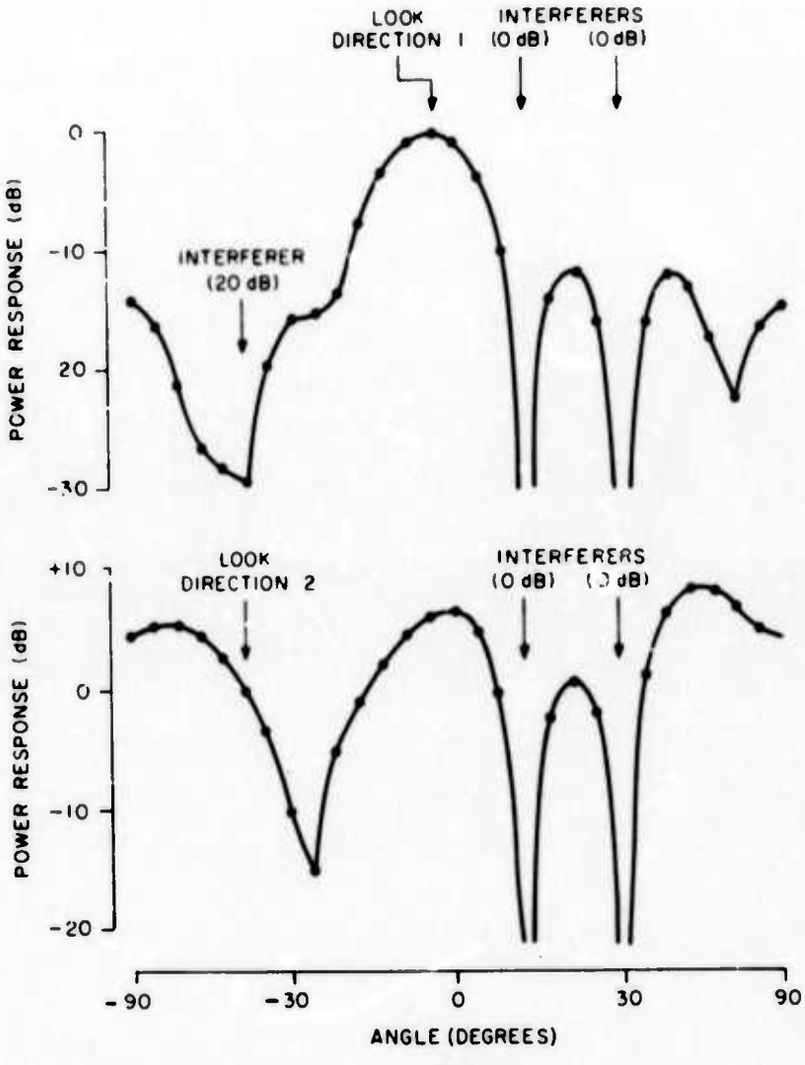

(b)

Figure 4. For a Seven Element, Uniformly Spaced Array, (a) Weight Magnitude versus Element Number, (b) Fixed Weight Patterns for the Two Look Directions Indicated by Arrows.

interferers as the desired look direction is changed.

2. The depth of the antenna pattern nulls are related to the signal strengths of the corresponding discrete interferers. Deeper nulls are placed on the stronger interferers.

3. The adaptive array patterns typically have a response maximum near the desired look direction.

4. The adaptive array response patterns are not "superdirective". Their "main beam" widths are similar to those of a uniform filled conventional array. Also, the very high (e.g., 10^6) weight magnitudes characteristic of super gain schemes have not been observed.

5. The adapted weight values increase for look directions in the vicinity of discrete signal components of high SNR.

3.1.2 Adaptive Versus Conventional Maps of the Environment

The concept of an array pattern, while still valid, is of limited usefulness in describing the performance of adaptive processors used to scan the environment (say to map the location of interferers or to search for weak target echoes). In contrast to the patterns of conventional beamformers which remain constant (in sine space) as the look direction is scanned, the pattern of an adaptive array is different for each look direction, there may or may not be a "main beam" and it may or may not point in the desired look direction, and the peak sidelobe level of the pattern for any given look direction is a poor indicator of how serious the effects of strong interferers will be when the beam is steered elsewhere. It will be more useful to think of the adaptive

processor as an estimator of the power arriving from a given direction and to ignore the details of the pattern formed in order to obtain that estimate. This section will compare the quality of that estimate for conventional and adaptive beamformers.

Figure 5 compares the sky maps (signal intensity versus angle) obtained by scanning the environment with a conventional beamformer (top) and an adaptive beamformer (bottom). The array and the environment are the same as illustrated in Figure 3. The conventional beamforming was done with uniform weights (no taper). Arrows indicate the position of the discrete signal sources. The conventional map suffers from two problems: the two strong sources are not well resolved and the existence of the weak signal is masked by sidelobe responses from the two strong signals. These problems are not present on the adaptive map. The two strong sources are well resolved and the weak source is clearly visable. The adaptive processor has made better use of the information available from the array elements in estimating the characteristics of the environment. The improvement can be described by saying that the effective beamwidth of the array has been narrowed and that the effective sidelobe level of the array has been reduced, if it is kept in mind that the array pattern for any given look direction does not exhibit these properties (e.g., Figure 4).

A second comparison between sky maps produced with conventional and adaptive processors is shown in Figure 6. In this case a 40 dB Dolph taper has been applied to the conventional array in order to suppress sidelobes. It is quite effective in doing so but at the cost of broadening the main beam and thus making the problem of resolving the two strong sources worse. The adaptive map is shown as before for comparison. Not only are the sources better resolved in the adaptive display but the noise floor between sources is

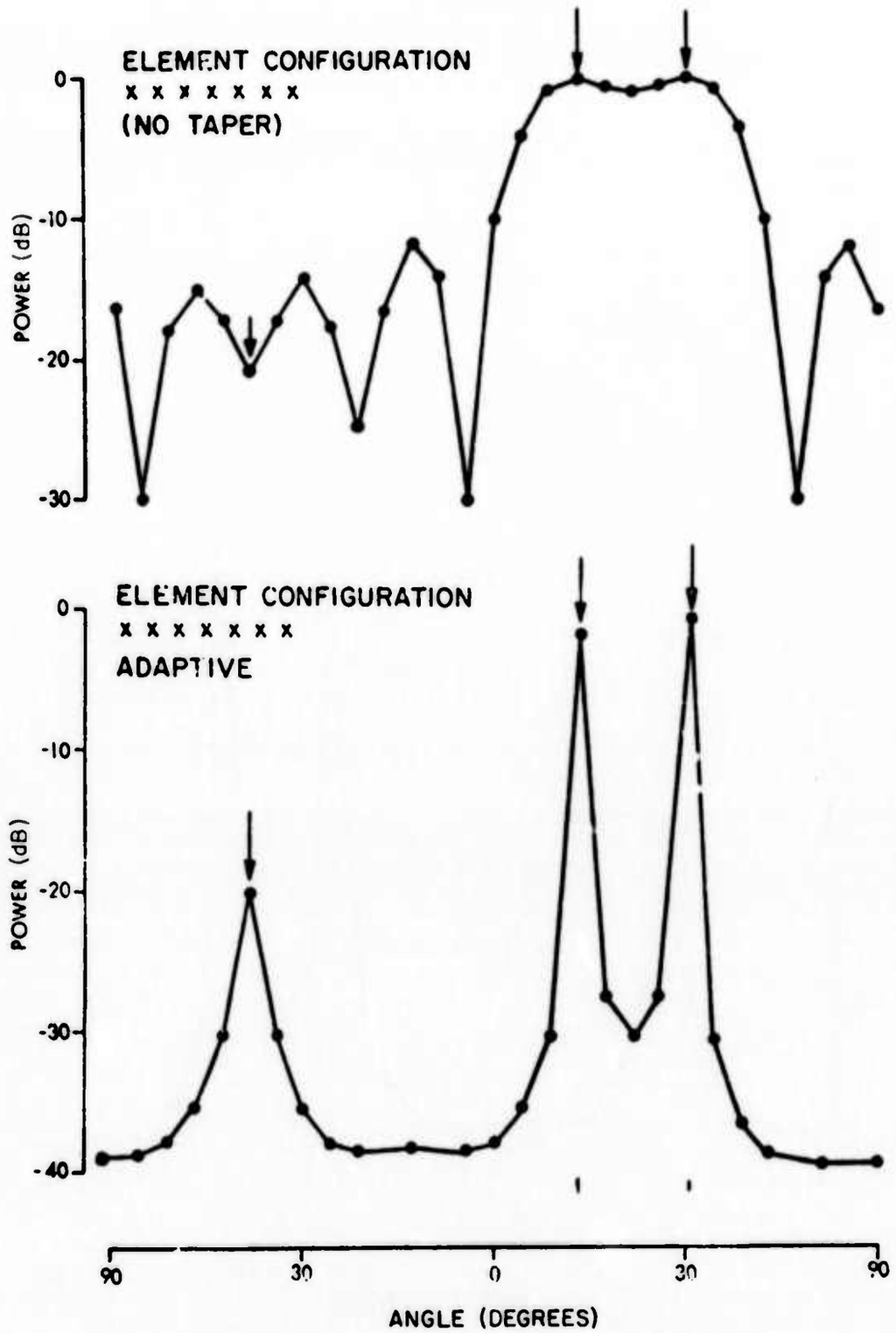

Figure 5. Comparison between the Performance of a Conventional Beamformer with Uniform Weights (top) and an Adaptive Beamformer (bottom).

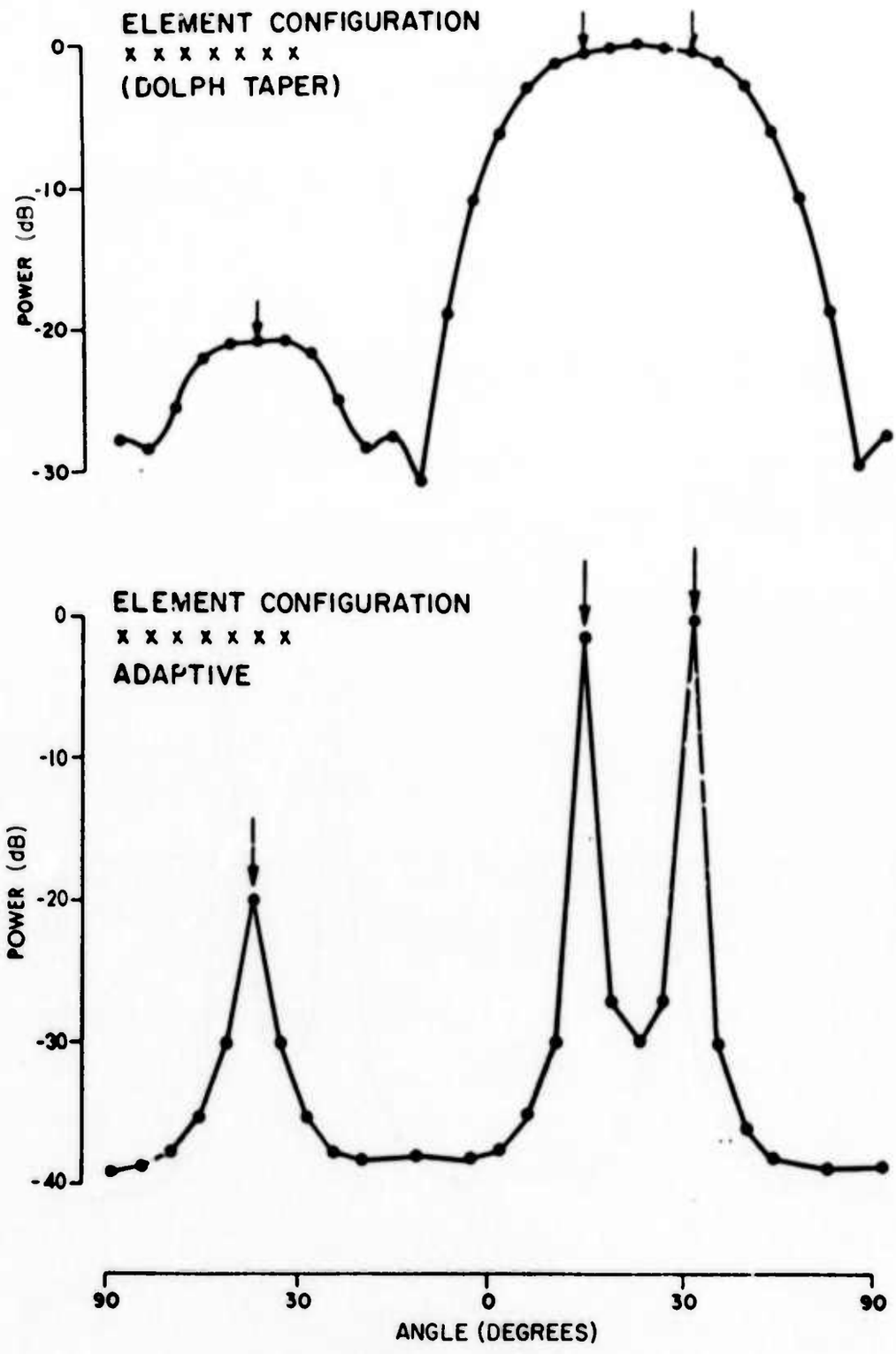

Figure 6. Comparison between the Performance of a Conventional Beamformer with Dolph Weights (top) and an Adaptive Beamformer (bottom).

significantly lower.

The improvement in SNR achieved by applying adaptive processing instead of conventional processing (with uniform weights) to the array and environment shown in Figure 3 is plotted as a function of look direction in Figure 7. This is the difference between the two curves shown in Figure 5 and illustrates that the improvement obtained varies greatly from one look direction to another. No improvement is obtained when looking directly at discrete sources and little improvement is obtained in directions such that the nulls between the sidelobes of the conventional pattern straddle the strong interferers.

These examples illustrate the features which characterize adaptive processors and make them potentially attractive for HF radar and communications applications. These examples are of course special cases and care must be exercised when extrapolating to other situations because the performance achieved will depend upon both the array and the environment.

3.2 ADAPTIVE PROCESSORS WITH SPARSE ARRAYS

Simulations have been used to study the impact of element placement (array geometry) on the performance of an adaptive processor. The primary motivation for this study was the need to choose a specific array geometry for installation in the field to collect the program data base. The objectives of the data collection were

1. to map the environment so as to define the strength and position (azimuth and elevation) of interferers,

and

2. to evaluate the improvement (e.g., noise floor reduction) achieved, as a function of position relative to the interferers,

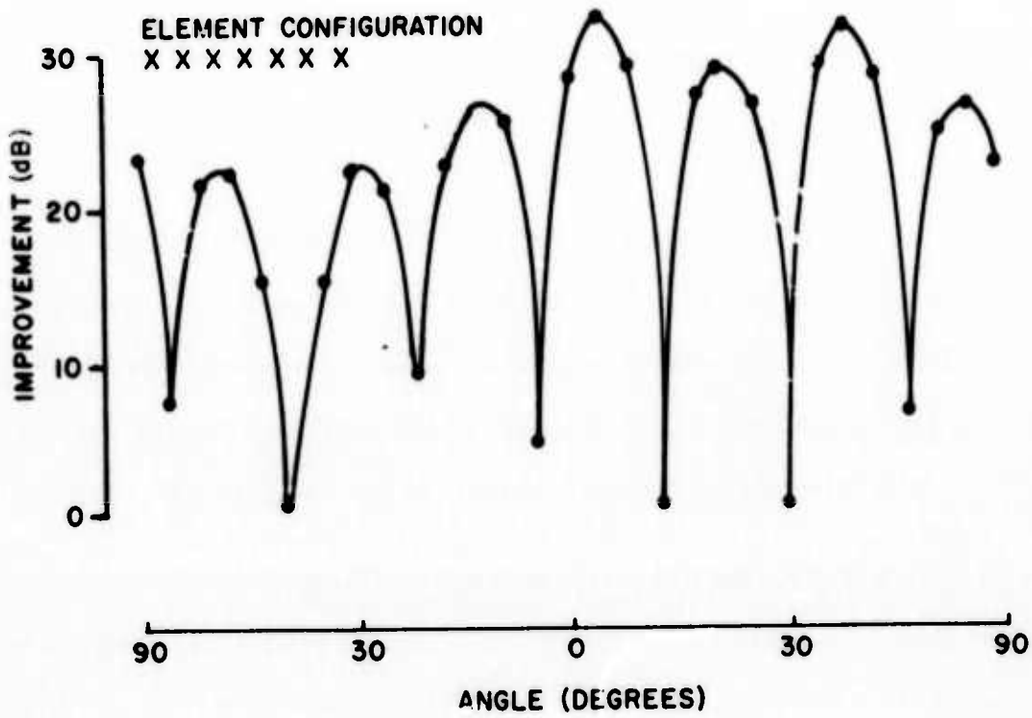

Figure 7. Improvement in SNR through Adaptive Processing Rather than Conventional Processing with Uniform Weights.

by processing the array adaptively rather than conventionally.

The constraint was that only 32 elements (and their associated receivers and processing equipment) could be afforded within the program budget and the problem was to distribute these in two-dimensions so as to optimize the performance of the array. The choice then was between a small filled array or a large sparse array. In conventional beamforming the small array gives better sidelobe performance but poorer angular resolution.

It was first recognized by radio astronomers that both high angular resolution and low sidelobe levels could be achieved at the same time for a special class of sparse arrays (low redundancy arrays) if special processing techniques were employed (Reference 4). The basis for this approach is the fact that the intensity of the angular spectrum (the sky map) can be otained either by taking the Fourier transform of the aperture distribution and squaring the magnitude of the result (this is the software implementation of conventional processing) or by first computing the autocorrelation function across the aperture (correlation coefficient versus interelement spacing) and Fourier transforming this. The significance of this is that it shows that all the sky map information of interest is contained in the measured autocorrelation function for the environment: each point on the autocorrelation function represents a different inter-element spacing in the array and (for averaging times long enough so that the incident signals become incoherent with each other) the result for a given spacing is the same no matter which pair of elements at that spacing is used. This means that elements of a filled array can be removed so long as all the spacings present in the original filled array still occur at least once. The elements saved in this way can be added outside the boundary of the original filled array so as to make available large

inter-element spacings not present at all in the original array. Ideally, array configurations could be found for which all spacings occur only once: such arrays are called non-redundant or zero-redundancy arrays but exist only for arrays of four elements or less. For larger numbers of elements some spacings occur more than once and these are called low-redundancy arrays. The configuration which gives the lowest number of redundant spacings for a given number of elements is called a minimum redundancy array. In any event, the processing procedure is to compute the autocorrelation function for the array, weight this function to control sidelobes (as one would weight the physical aperture in conventional processing to control sidelobes), and Fourier transform the weighted autocorrelation function to obtain the sky map. The key point is that it is the autocorrelation function for the array which must be filled, not the physical aperture: the physical array can be made sparse while maintaining low sidelobe levels by applying weights to the autocorrelation function rather than to the physical aperture. The array can be thinned until further element removal would cause a "hole" in the autocorrelation function (a spacing not represented in the array).

If mapping of the interference environment had been the sole purpose of this program, a sparse, low-redundancy array would have been the obvious choice with processing and sidelobe control done non-adaptively in the autocorrelation domain. It was not obvious that such arrays would also be suitable for adaptive processing but it seemed plausible that this would prove to be the case for the following reason: adaptive processors have the property that they try to adjust the pattern of the array so that the sidelobes don't fall on strong interferers. Even when used with filled arrays capable of low pattern sidelobe levels, adaptive processors characteristically produce patterns with

high sidelobes because it is often preferable from an SNR viewpoint to have high sidelobes pointing in quiet directions in order to obtain deep nulls in just the right direction to reject strong discrete interferers. That is, pattern flexibility is more important than peak sidelobe level. The fact that sparse arrays have high peak sidelobes does not, therefore, necessarily disqualify them as effective adaptive arrays, particularly when the elements saved by making the array sparse are used to make the overall dimensions of the array larger and thus to give the adaptive processor new and longer baselines to work with.

A series of simulations were done to study the performance of low redundancy sparse arrays under adaptive processing. The first case illustrated compares the performance of a filled seven element array to a sparse four element array of the same aperture. The filled array and the environment is the same as that shown in Figure 3. The sparse array is formed by removing elements number 3, 5, and 6: the resulting array has all the interelement spacings of the filled array. Figure 8 compares the performance of this array (top) with the performance of the filled array (bottom) under adaptive processing. The filled array does a better job of maintaining a uniformly low noise floor but the source resolution achieved with both arrays is comparable (not surprising, since the aperture is the same) and the sparse array with adaptive processing is much superior to a filled array of the same aperture with conventional processing (uniform weights, top of Figure 5: Dolph weights, top of Figure 6). The upshot of this is that one buys improved adaptive performance by filling in a sparse array at the cost of additional elements and processing load.

A situation for which the result is harder to anticipate is one in which a fixed number of elements are available and the question is whether to

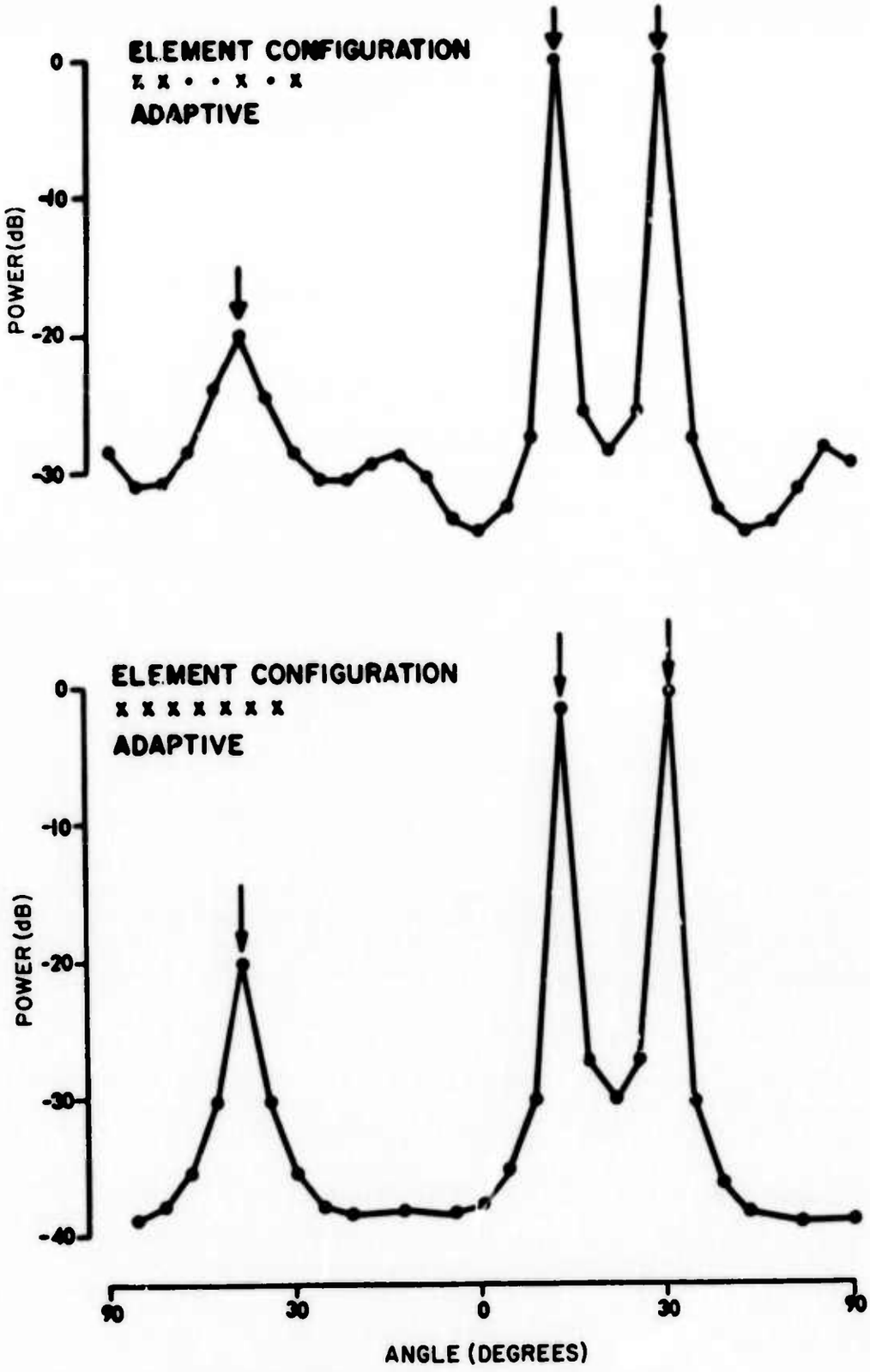

Figure 8. Comparison between the Adaptive Performance of a Sparse Array (top) and a Filled Array of the Same Aperture (bottom).

distribute these to form a small aperture filled array or a larger aperture sparse array. This case is illustrated in Figure 9 where the adaptive performance of a nine element filled array (top) is contrasted with a nine element sparse array (bottom). The elements of the filled array are spaced by a half wavelength, making the overall aperture of the array four wavelengths wide. The first three elements of the sparse array are spaced by a half wavelength but the remaining six elements are spaced by one and a half wavelengths, making the overall aperture of the sparse array 10 wavelengths. This sparse array has all the inter-element spacings present in a filled 10 wavelength array. The environment used for these simulations is the same as that in Figure 3. The result is that the effective angular resolution of the sparse array is better and the noise floor away from discrete sources is somewhat poorer. The effective angular resolution of the sparse array is better than that of the filled array by roughly the ratio of the array apertures (e.g., the discrete sources appear 2 to 3 times as wide 35 dB down for the filled array than for the sparse array). The noise floor for the sparse array averages a few dB higher than that for the filled array, however.

The results illustrated to this point have been for small one-dimensional arrays in order to make the displays simple and the results easy to grasp. Similar results have been obtained for larger two-dimensional arrays of the type intended for data collection in this program.

The cross is a two-dimensional example of a low-redundancy sparse-array: a filled array of the same aperture would require an additional 240 elements, receivers, and processing channels and economically would be out of the question. A 32 element filled array in two-dimensions would have a third the angular resolution of the cross in both azimuth and elevation and would offer no important advantage in noise floor reduction. Figure 10 is a

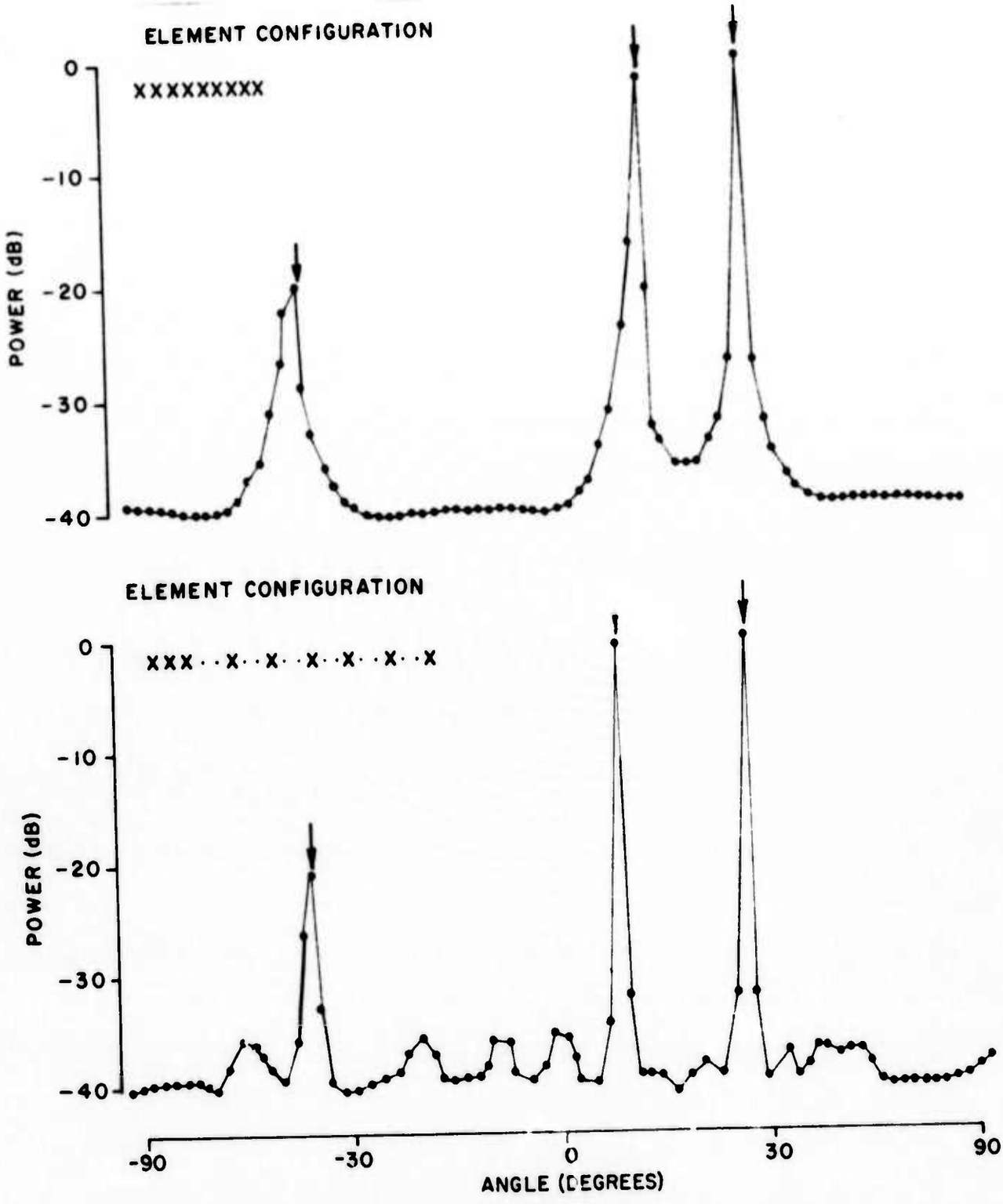

Figure 9. Comparison between the Adaptive Perfc mance of a Sparse Array (bottom) and a Filled Array of the Same Number of Elements (top).

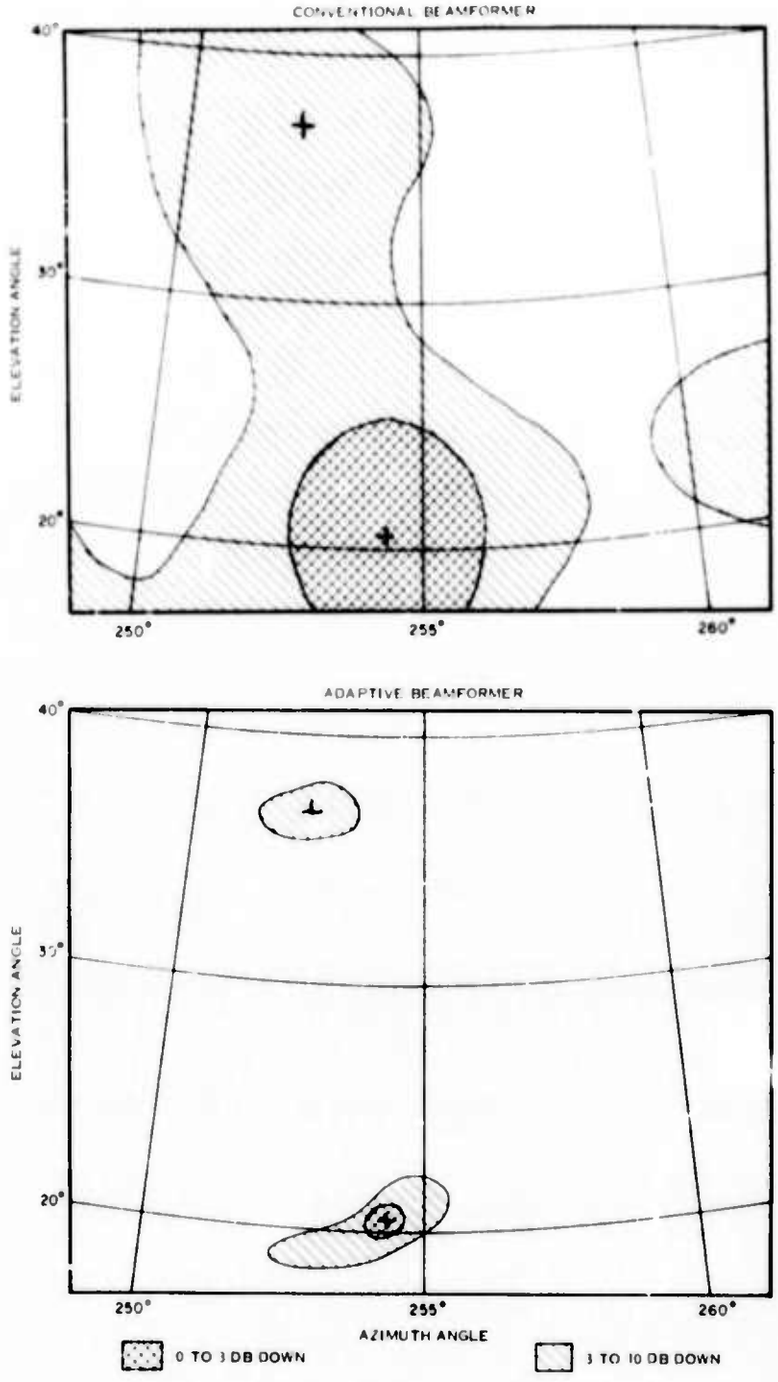

Figure 10. Simulated Conventional (top) and Adaptive (bottom) Sky Maps for a 32 Element Cross Array. The Environment Consists of Two Discrete Sources of Unequal Strength and an Omni-Directional Noise Background.

simulation for the 32 element cross comparing the performance of this array with conventional beamforming (top) and with adaptive beamforming (bottom). These maps are formed by computing the beamformer output for a 20 by 20 grid of discrete azimuth - elevation look directions then drawing contours of constant beamformer output through the results. The environment consisted of a discrete "low angle" signal of 0 dB intensity (lower cross on figure), a discrete "high angle" signal of -6 dB intensity (upper cross on figure), and an omni-directional noise background producing a signal of -5 dB intensity at each element. The display is a radio map of the sky in which strong signals are shown by double cross-hatching (signals within 3 dB of the strongest observed) and weaker signals by single cross-hatching (signals 3 to 10 dB below the strongest observed). With conventional processing the low angle signal appears as a broad circular region about 4 degrees in diameter (the 3 dB beamwidth of the main lobe), surrounded by a diffuse sidelobe region (single cross-hatching). The existence of the high angle signal is masked because when the beam is pointed in that direction, the sidelobes of the pattern fall on the stronger source. In the adaptive map, the position of the strong low angle source is much better localized (diameter of the 3 dB contour is about a sixth as large), sidelobe responses no longer appear, and the weak high angle source can be clearly seen.

These simulations suggest that sparse arrays are well suited for use with adaptive processors, particularly in situations in which the objective is not simply to detect a signal (maximize SNR) but also to tell where it is coming from (e.g., OTH radar or passive HF direction-finding applications). There are an infinity of ways in which a filled array can be made sparse: we have chosen to work with a particular class of sparse arrays (low redundancy) in which the array is thinned to the point where further thinning would

eliminate one or more inter-element spacings present in the parent filled array. The advantage of this particular class of sparse arrays for the program is that the option is preserved for producing high resolution maps of the environment by well established deterministic beamforming methods (Fourier transform of the weighted autocorrelation function for the array) for comparison with maps of the same environment produced by adaptive beamforming.

4.0 FIELD INSTALLATION AND DATA COLLECTION

A key objective of the program has been to collect data in the real HF environment and use it to evaluate the benefits of adaptive processing over more conventional techniques. The data for this purpose were collected at an established DARPA field site near Hudson, Colorado. Land, power, shelter, and much of the electronics required were already available at this facility as a result of other closely related programs. The additions and modifications made to this facility for collecting a data base for adaptive processing are described below.

4.1 FACILITY MODIFICATIONS

4.1.1 Vertical Monopole Flements

A large circular array (32 elements, 600 meter diameter) was available at the Hudson site and consideration was given to using thir array without modification. This proved not to be an attractive option because the elements of the circular array were horizontal crossed dipoles designed for receiving signals from the overhead ionosphere. These elements were not effective at the low elevation angles of practical interest in most potential applications of adaptive processing (e.g., over-the-horizon radar). The principal requirement of the data base we were to collect was that it be representative of the HF environment under conditions of practical interest and consequently it was decided to build 32 new elements better suited to the task. A vertical monopole element design was available which had been used with success at low elevation angles in other applications. The radiating element is electrically short (5 feet) to

make it broadband and thick (1 foot) to reduce the base impedance. A high impedance base amplifier provides gain (18 dB) and impedance matching to the transmission line so as to maintain an acceptable system noise figure over the HF band (3-30 MHz). A set of 32 of these elements were built and installed within the existing circular array. A sketch of the installation and the array elements is shown in Figure 11. The bottom of the vertical radiating element was mounted about three feet above ground level so that the base amplifier could be inspected with snow on the ground.

4.1.2 Cross Array Geometry

The cross array is a familiar example of a low-redundancy two-dimensional array. It has the virtue that the elements are equally spaced along orthogonal axes (in contrast to a circular array) which simplifies the processing software. It also has the property that the data from the elements in either leg can be used alone to study the performance of a one-dimensional array of the same aperture as the parent two-dimensional array. For these reasons the cross array was chosen for use in the program. A sketch of the installed array is shown in Figure 11 and a dimensional plan view is shown in Figure 12. The inter-element spacing is 20 meters (a half-wavelength at 7.5 MHz). The east-west leg of the array is 16 elements long (a 300 meter aperture) and the north-south leg is 17 elements long (a 320 meter aperture).

4.1.3 Receiving and Data Acquisition System

The receiving and data acquisition system used to collect the adaptive data base is shown in Figure 13. The new instrumentation required to assemble this system from the equipment already available at the Hudson site was

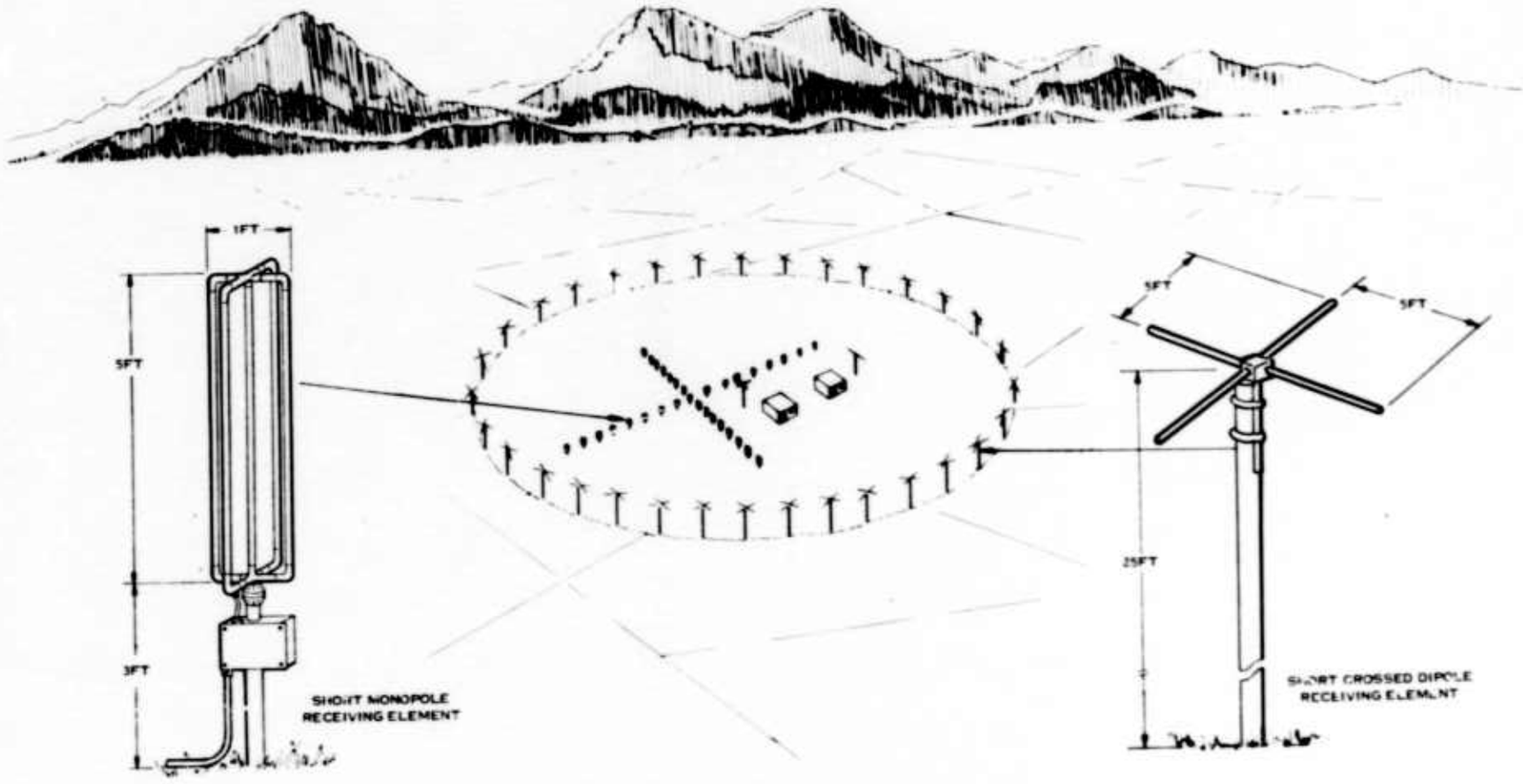

Figure 11. Artist's Sketch of the Hudson, Colorado Field Site: The Cross Array was Used for the Data Collection Portion of the Program.

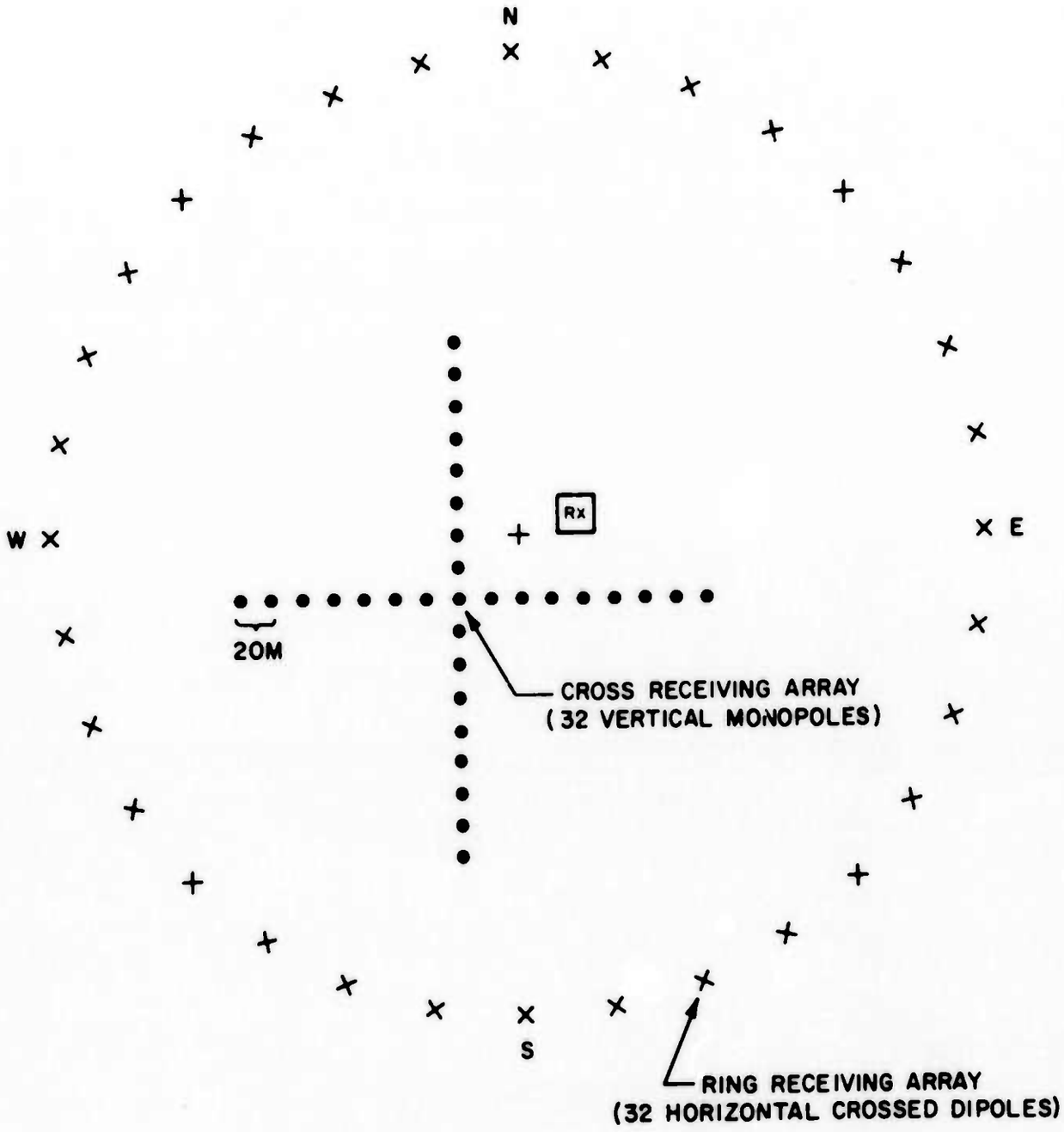

Figure 12. A Plan View of the Hudson Field Site Showing the Orientation and Inter-Element Spacing of the Cross Array.

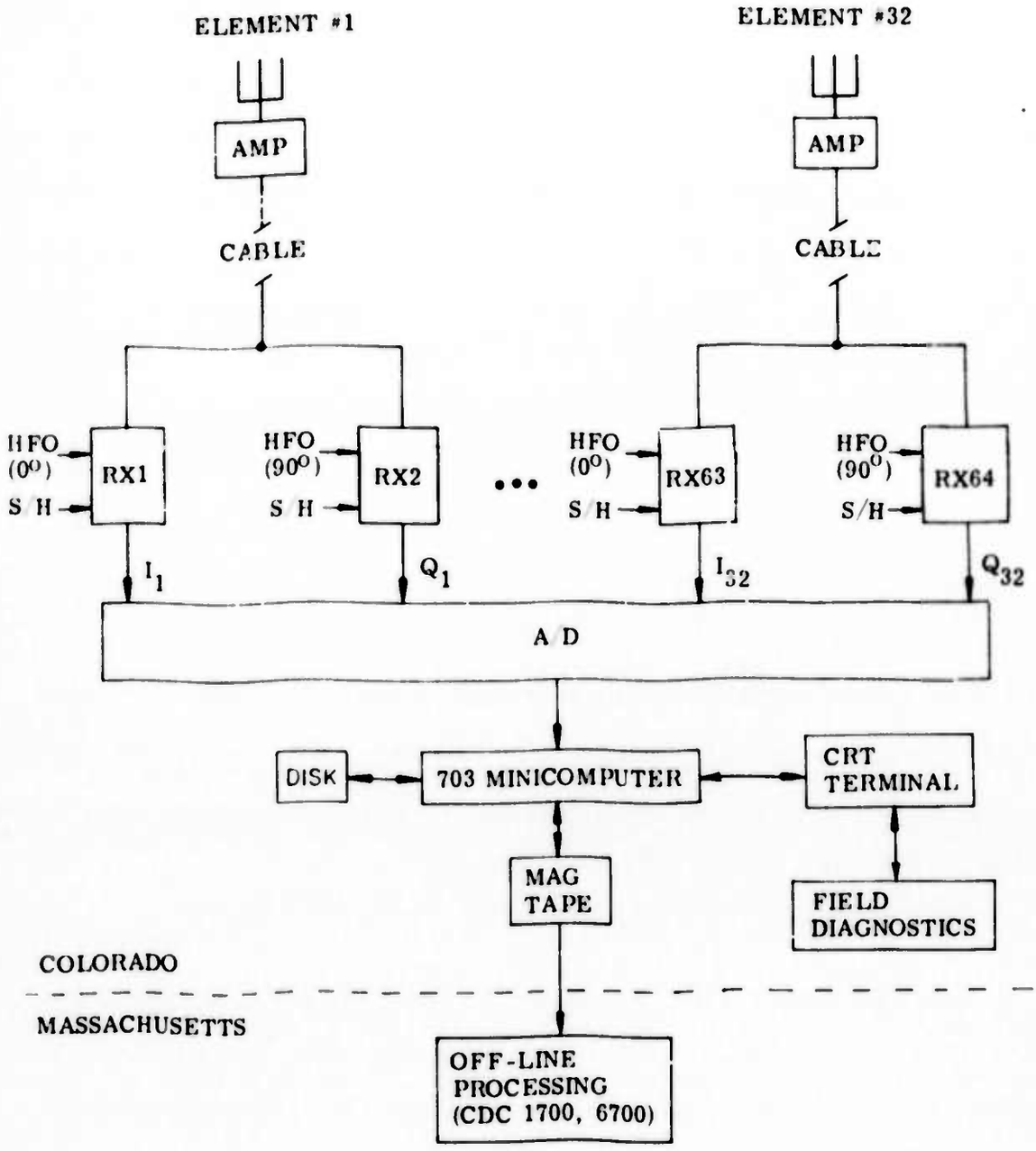

Figure 13. A Block Diagram of Cross Array Electronics and Associated Data Acquisition System.

a set of 32 "Q" receiver modules, the associated power dividers, and the HFO distribution circuitry. These receivers are identical to the original set of 32 but the HFO signal is shifted by 90°. A pair of receivers is used for each element, providing the complex samples required for adaptive processing. The 64 receiver channels are all sampled simultaneously and the results held while an A/D converter steps from channel to channel and transfers the data to the minicomputer memory (dish storage). The process is repeated periodically until the computer memory is full: data collection then stops while the stored information is recorded on digital tape (four minutes required to accomplish this). The memory will hold 90112 words which corresponds to 22 blocks of data, each block containing 64 time samples of the entire array, each sample being a set of 64 receiver channel voltages. The data base for this program was collected at the rate of 50 samples of the entire array per second. This corresponds to one data block every 1.28 seconds and the 22 block capacity of the memory in 28.16 seconds. The data acquisition sequence thus alternated between half-minute periods of data collection and four minute periods of data recording.

4.2 TEST GEOMETRY

Data were collected with and without cooperative CW transmissions from an SRI field site at Lost Hills, California. The SRI transmissions provided signals under realistic but controlled conditions and it is only data from this portion of the data base which have been analyzed in this report. The geometry of the path from Lost Hills, California to Hudson, Colorado is shown in Figure 14. The length of the path is 1433 km and the azimuth (measured from Hudson) is 254.5 degrees.

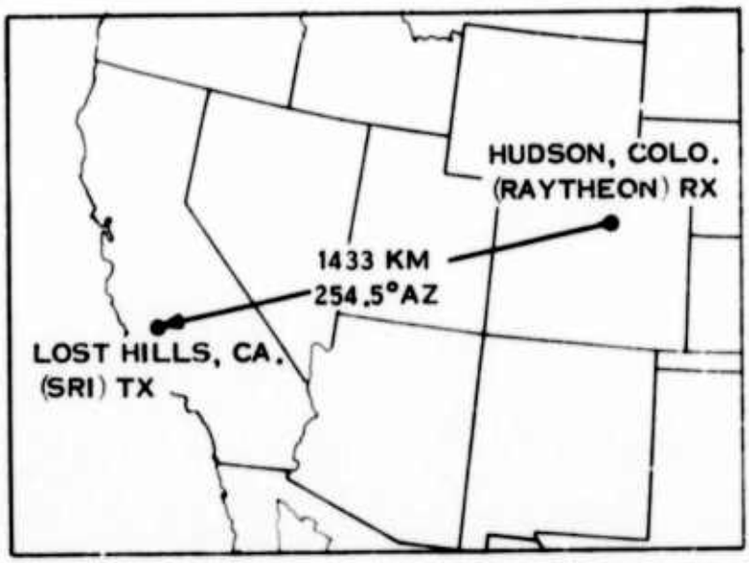

Figure 14. Geometry of Cooperative Tests with SRI Providing a Controlled Interfering Signal.

4.3 DATA COLLECTION

The purpose of the data collection effort was to obtain a sampling of the HF environment over a range of frequencies and interference conditions. Table 1 summarizes the environmental data on tape.

TABLE I: ENVIRONMENTAL DATA BASE

Date	Freq.	Environment	Records*
18 Nov. 1973	7 MHz	Amateur Radio Band (heavy, multiple source interference)	44
19 Nov. 1973	10 MHz	Cooperative SRI Transmissions (multiple hop, element SNR >1)	176
	15 MHz	Cooperative SRI Transmissions (single hop, element SNR >1)	176
	15 MHz	Cooperative SRI Transmissions (single hop, element SNR <1)	176
28 Jan. 1974	15 MHz	International Broadcast Band (heavy, multiple hop interference)	924

* Each data record contains 64 complex samples of each array element and represents 1.28 seconds in time.

5.0 ANALYSIS OF EXPERIMENTAL DATA

5.1 SIGNAL ENVIRONMENT

The data analyzed in this section was taken as reprcsentative of the least complex adaptive environment likely to be encountered in practice, a strong CW interferer arriving via a single hop path. The interfering CW signal was provided by SRI (see Figure 14 for test geometry) at a frequency of 15.729 MHz. This frequency was chosen so as to be just below the maximum usable frequency (MUF) for the path at the start of the data taken to insure that only one-hop signals would be observed. The one-hop signal will of course be composed of high and low angle, ordinary and extraordinary modes but by operating near the MUF we hoped to minimize their angle of arrival differences and obtain an incident signal on the array which approximated a single point source in the far field. Such a source would produce a plane wave incident on the array, a common assumption in numerical simulation studies of adaptive processors and therefore an important situation to study experimentally. Ionospheric conditions were such that the SRI signal arrived at the array at an elevation angle of about 15 degrees and at an azimuth angle of about 254 degrees. The SNR in the full 17 kHz bandwidth of the receiver was of order 10 dB (measured at the element, prior to array gain).

5.2 ONE-DIMENSIONAL RESULTS

The simulations presented in Section 3.0 emphasized one-dimensional arrays because the results from such arrys are more convenient to display in detail and because the concepts involved are qualitatively the same in

either one dimension or two. One of the advantages of collecting data on a cross array is that the outputs from one leg at a time can be processed after the fact to give results for a one-dimensional array and this has been done for comparison with one-dimensional simulations. Since the SRI signals arrive from the west, the north-south leg of the array was used to form a 17 element broadside array and subsets of this array were processed for comparison with the simulations. The results for a 1.28 second data block are shown in Figure 14. The plot at the top of this figure shows the power output of the adaptive signal. This result is for an array of 15 elements spaced 20 meters apart. The 3 dB conventional beamwidth of the array (at 15.729 MHz) is 4 degrees and this angular width is indicated on the figure at the 3 dB down level. As anticipated from the simulations (Figures 5 and 6 of Section 3.0), the definition of the position of the discrete source is much sharper with adaptive processing than with conventional (by a factor of about 15 at the 3 dB down level in this example). The sidelobe responses are well below the 13 dB down level expected for conventional processing. The plot at the bottom of this figure shows the result of removing 9 of the original 15 elements of the one-dimensional array to form a sparse array of nearly the same aperture but less than half the number of elements. As anticipated from the simulations (Figure 7 of Section 3.0), the angular width of the discrete source is essentially the same for the sparse array as for the filled array. The conclusion is that the simulations have proven to be in satisfactory qualitative agreement with results obtained in the real HF environment.

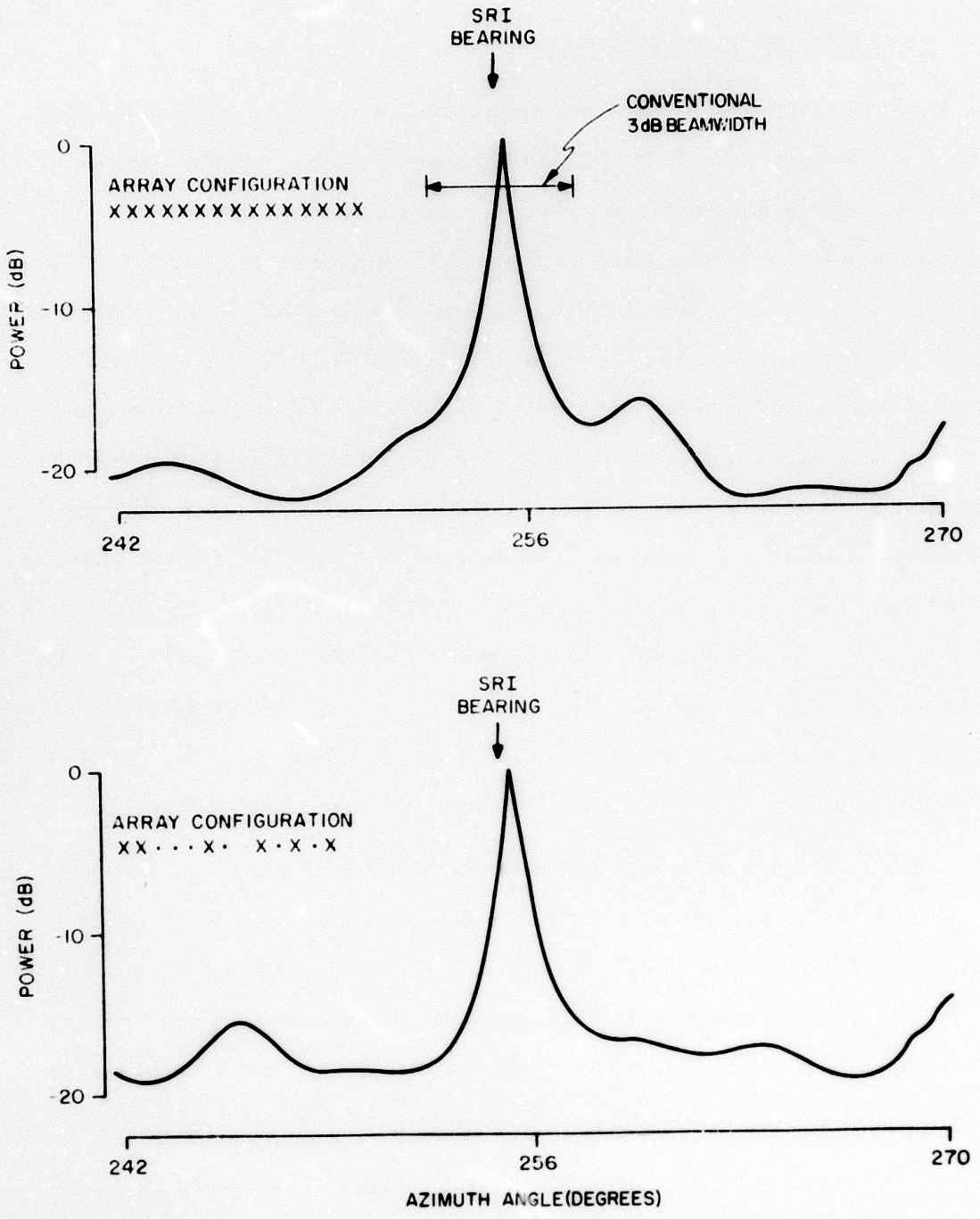

Figure 15. Comparison of Azimuth Maps of SRI Signal (15.729 MHz) with Filled Array (top) and Sparse Array (bottom). The Sparse Array has fewer elements but Comparable Aperture.

5.3 TWO-DIMENSIONAL RESULTS

An attractive feature of a two-dimensional array for a study of adaptive processing performance is that it permits one to map the radio sky to show where the interfering signals are coming from and then to show how the noise floor reduction varies as a function of position relative to these signals. The noise floor reduction is thus not presented as a single number but rather as a contour map showing the improvement in the noise floor as a function of azimuth and elevation in the sky. We have called this display an "improvement" map. The improvement in the noise floor achieved in a given direction is the difference between the power output of the conventional processor and power output of the adaptive processor. The improvement map is a contour plot showing how the noise floor reduction varies as a function of azimuth and elevation across the radio sky. Since the conventional, the adaptive, and the improvement map are closely related we have displayed them together as a set for each data block, along with a plot of the frequency spectrum of the received signal from which the element SNR for that data block can be read.

The SRI signal was characterized by a fading period of about 5 seconds: a 1.28 second block length was short enough so that the signal level did not change significantly over that interval. In order to examine conditions over a range of signal levels a series of 11 contiguous data blocks were processed, corresponding to about 14 seconds in time and covering about 3 fading periods.

Results for the first data block are shown in Figure 16. The azimuth and elevation scales for the three maps are the same and show the sector of the sky containing the interfer. The scales are linear in "sine-space", making them non-linear in angle in such a way that the foreshortening of the

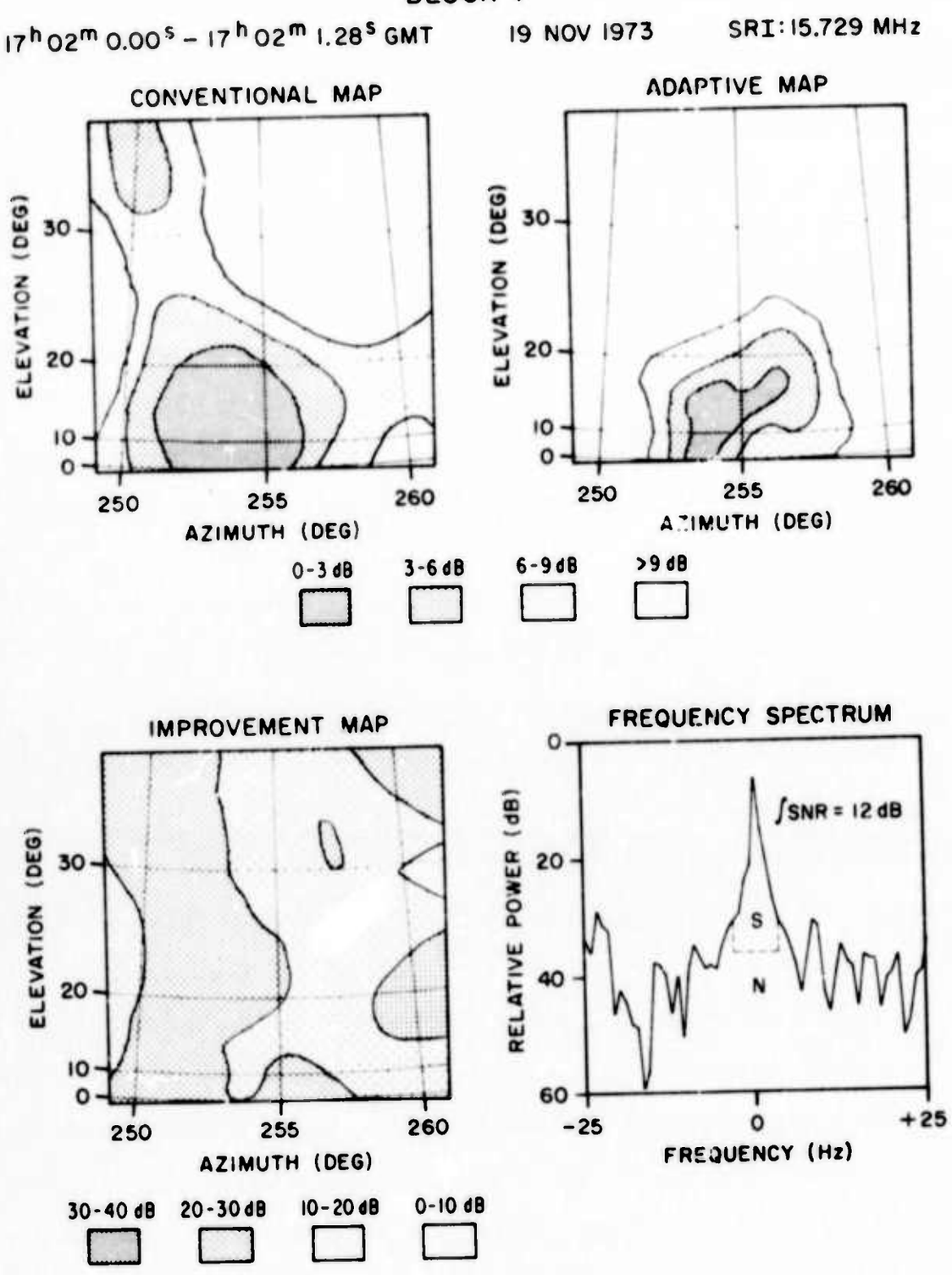

Figure 16. Conventional Map, Adaptive Map, Improvement Map, and Frequency Spectrum for Data Block Number 1.

aperture which occurs as the array is steered off-boresight (zenith) is compensated for on the display. The effect is to keep the shape of the antenna pattern constant on the display regardless of position and consequently make point sources at low elevation angles appear as round images rather than as elliptical images extended along the elevation angle axis. The conventional map shows the SRI signal at about 15 degrees elevation angle and about 254 degrees azimuth. Gray scales are used to show signal level. The darkest area represents the first three dB down from the peak signal and shows that the conventional half-power beamwidth of the array is about 5 degrees. The theoretical value for a true point source is 4 degrees: the slightly greater measured beamwidth is possibly due to the finite angular dimensions of the source. The peak sidelobe responses of the array are strongest along two orthogonal arms which mirror the geometry of the cross: the peak sidelobe level is of order 5 dB below the main beam response. This relatively high sidelobe level is characteristic of sparse arrays with conventional processing and would not be helped by applying a fixed set of weights (e.g., Dolph-Tchebyscheff) in the beamforming process. The sidelobes could be reduced by filling the array (requiring an additional 240 elements and receivers) and then applying a fixed set of weights but this would not improve the angular resolution. The adaptive map does not exhibit the high sidelobe responses of the conventional map and the "main beam" signal definition is somewhat better. It is probable that the signal at this time actually consists of two or more modes of comparable strength separated in angle (or perhaps a single mode "scintillating" in angle during the 1.28 seconds used to collect the data). The contours for the adaptive map have been drawn in terms of dB below the power level

obtained when the adaptive processor is steered in the direction of the interferer. This makes possible a direct comparison between the shapes of conventional and adaptive sky map patterns but it does obscure the fact that the maximum power output of the adaptive processor was 18 dB less than the maximum power output of the conventional processor in the source direction. For an ideal point source the two processor outputs should be the same and we tentatively attribute the discrepancy to the finite dimensions of the source: an equivalent statement is that the signal incident on the array departs significantly from a plane wave. The result is a lowering of the noise (interference) floor with the adaptive processor when steered in the general direction of the interferer, in contrast to simulation results based on ideal plane wave signals which predict no noise floor reduction when looking at the interferer. The improvement map itself shows noise floor reductions between 20 and 30 dB over much of the sky, though there are regions where little improvement is obtained. The SNR is an important parameter in the comparison of field data with simulations: we have estimated this quantity from the power spectrum of the signal using one receiver pair (I and Q channels for one array element). The signal energy is confined to within a few Hertz of the center frequency. The frequency bins outside this region have been taken as noise and used to compute an average noise level. It has then been assumed that this noise level is also representative of the noise level within the frequency bins containing signal (horizontal dashed line on the figure separating signal from noise). The total noise power and the total signal power across the spectrum have then been computed and these numbers used to compute the integrated SNR shown on the figure (12 dB). All of the noise power in the 17 kHz bandpass the receiver is represented in the displayed spectrum because of

aliasing into the ±25 Hz window displayed on this figure. The 12 dB SNR for data block # 1 is one of the highest of this series, even though the adaptive and the improvement maps are among the least impressive. This leads us to believe that variations in mode structure from map to map are playing an important role in the performance of the adaptive processor.

Data block #2 is shown in Figure 17 and is by all measures the least impressive examples of adaptive (or conventional) processing. The element SNR is the lowest observed (8 dB), the conventional map is poorly defined and has an uneven sidelobe structure, the adaptive map shows somewhat better signal structure definition and freedom from sidelobe responses, and the improvement map shows only modest noise floor reductions (10 - 20 dB across most of the sky).

Data block # 3 (Figure 18) exhibits the highest SNR observed in this series (13 dB), more regular sidelobe structure in the conventional map, the presence of a more compact signal structure on the adaptive map, and noise floor reductions in the 20 to 30 dB range on the improvement map.

Data block # 4 (Figure 19) is one of the best examples obtained of the benefits of adaptive processing at HF. The conventional map is regular, the adaptive map provides a much sharper picture of the interfering signal, and the improvement map shows noise floor reductions in the 30 to 40 dB range. The element SNR for this data block was not outstanding (10 dB).

Data block # 5 (Figure 20) is the best example of the sort of results which would have been expected from simulations with a single plane wave interferer. The conventional map exhibits the classical cross sidelobe pattern, the adaptive map shows a single, sharply defined source, and the improve-

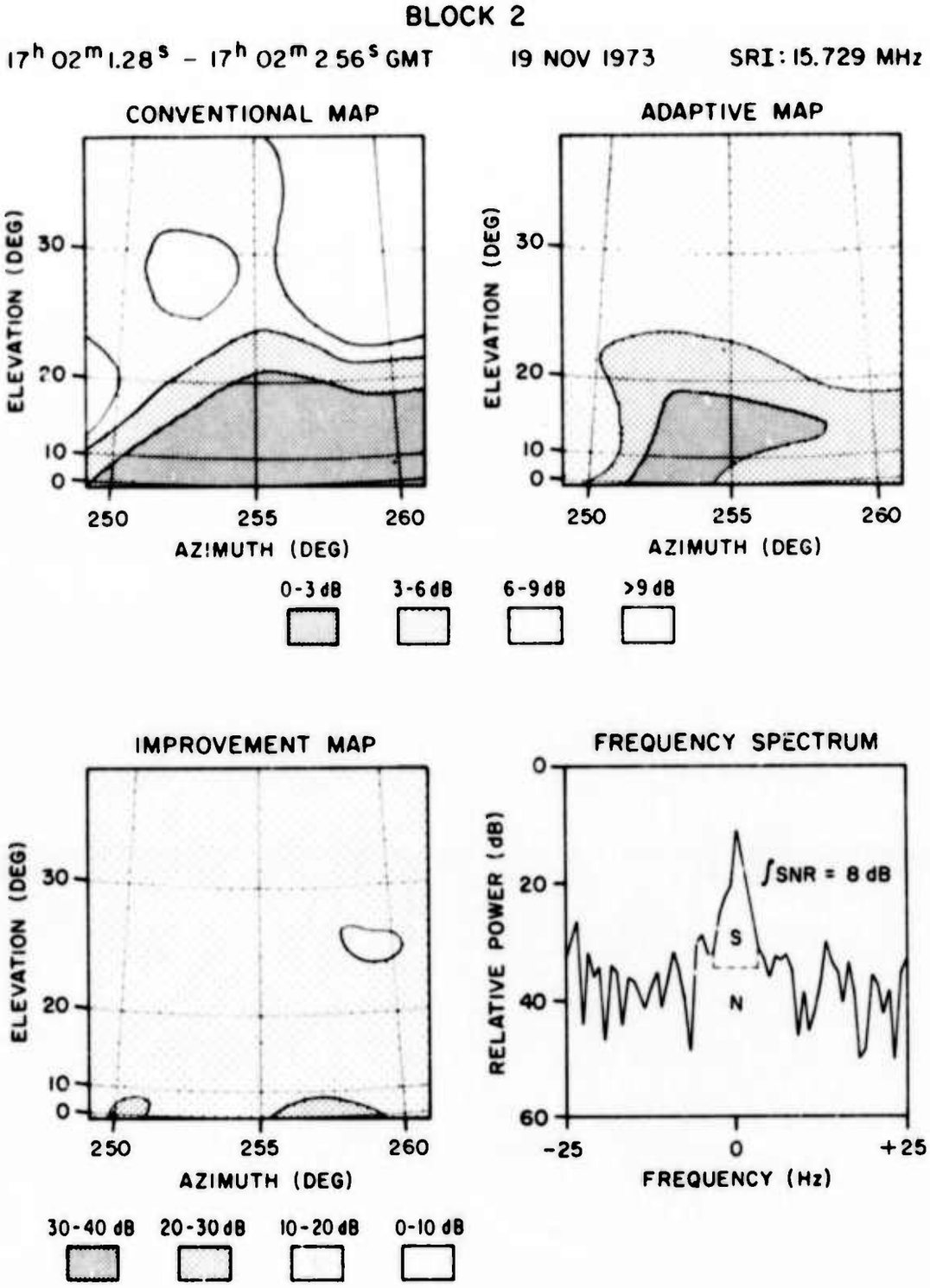

Figure 17. Conventional Map, Adaptive Map, Improvement Map, and Frequency Spectrum for Data Block Number 2.

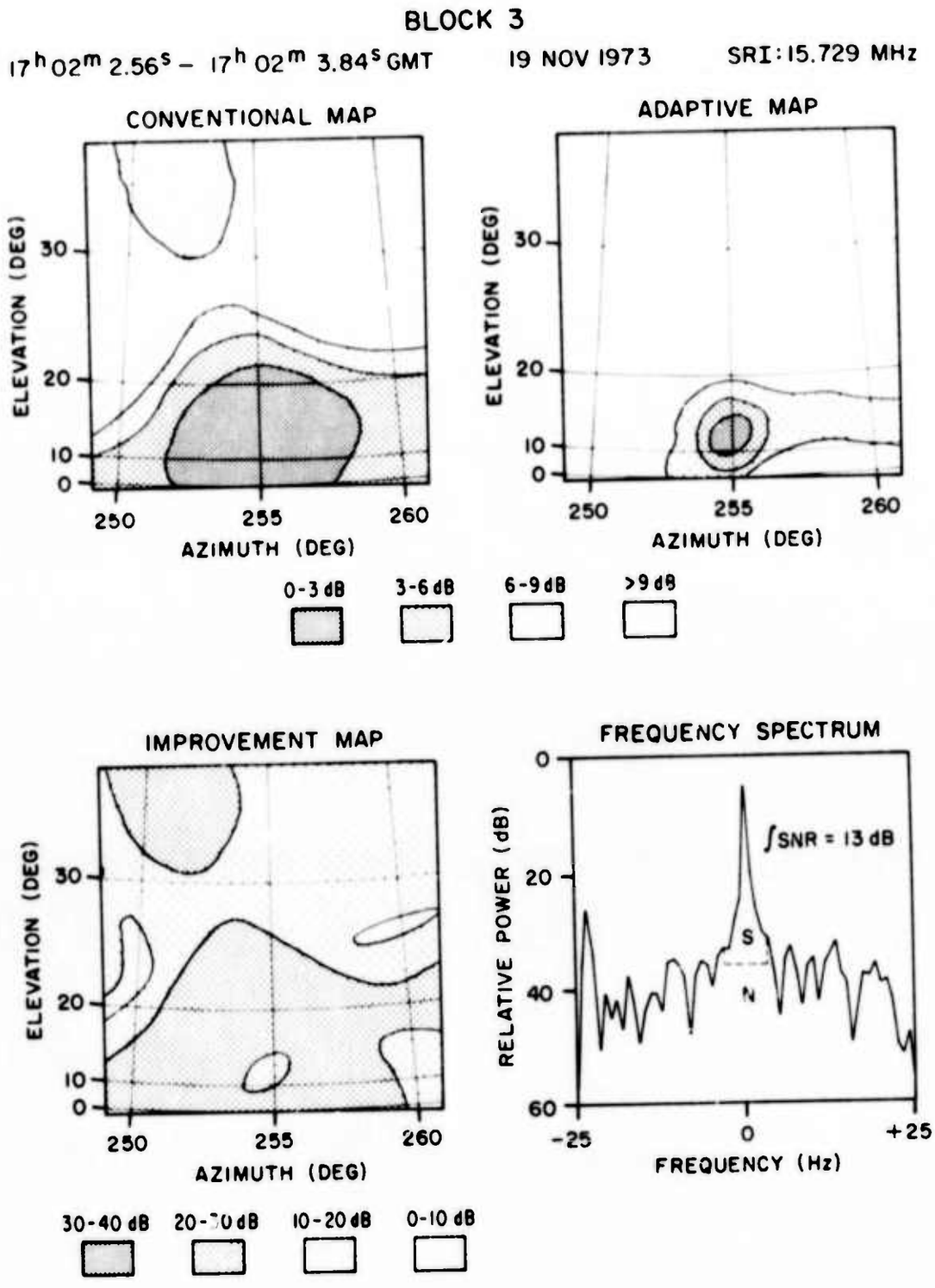

Figure 18. Conventional Map, Adaptive Map, Improvement Map, and Frequency Spectrum for Data Block Number 3.

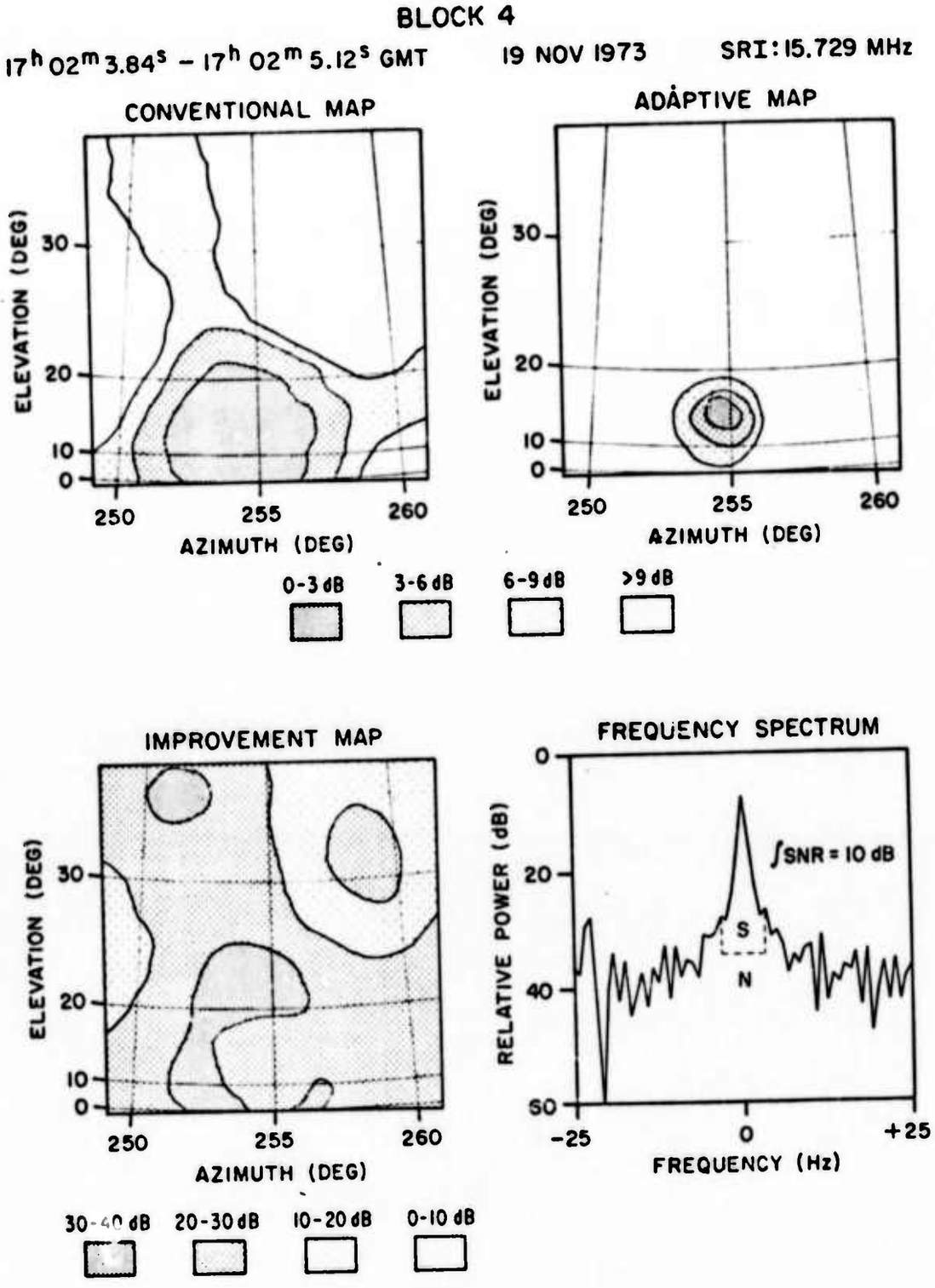

Figure 19. Conventional Map, Adaptive Map, Improvement Map, and Frequency Spectrum for Data Block Number 4.

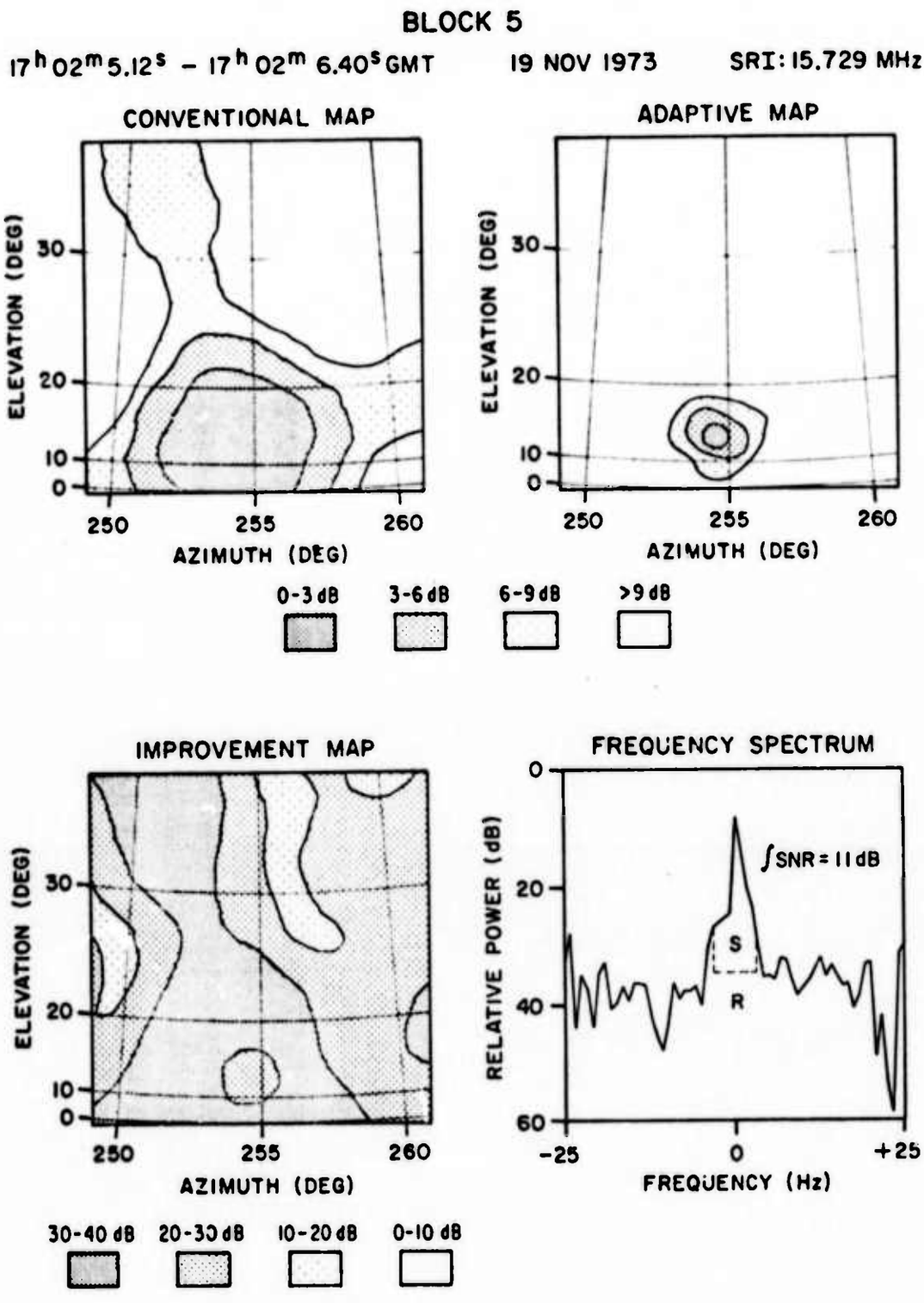

Figure 20. Conventional Map, Adaptive Map, Improvement Map, and Frequency Spectrum for Data Block Number 5.

ment map shows noise floor reductions of order 30 - 40 dB over much of the sky. The 3 dB width of the "main lobe" response on the adaptive map is about 6 times sharper than on the conventional map. This indicates that the interferer approximated a point source to within a degree of angular spread: the improvement map also shows the dip in improvement expected from simulations when the adaptive processor is steered in the direction of a point source interferer. Even here, however, the output of the adaptive processor is more than 20 dB below that of the conventional processor when pointed in the nominal direction of the interferer whereas simulations with an ideal point source interferer would predict equal output in both cases. The element SNR for this data block is 11 dB and thus is intermediate between the highest and lowest observed in this series.

Data block # 6 through # 11 (Figures 21 through 26) complete the series and are presented to show that while the details vary from block to block, the first 5 data blocks are representative of what can be expected under these conditions. These later data blocks are self-explanatory and no further discussion will be given.

To summarize, the preceding data set has shown that adaptive processing of two-dimensional HF arrays consistently produces improved definition of the angle-of-arrival, freedom from sidelobe responses, and significant noise floor reduction compared to conventional processing. The absolute magnitudes of the improvements are of course dependent upon the particular antenna array used and the particular set of field data chosen for analysis. The importance of what has been accomplished is that it has been shown that simulations using existing algorithms are satisfactory in most respects for predicting the performance of two-dimensional adaptive processors in the real HF environment.

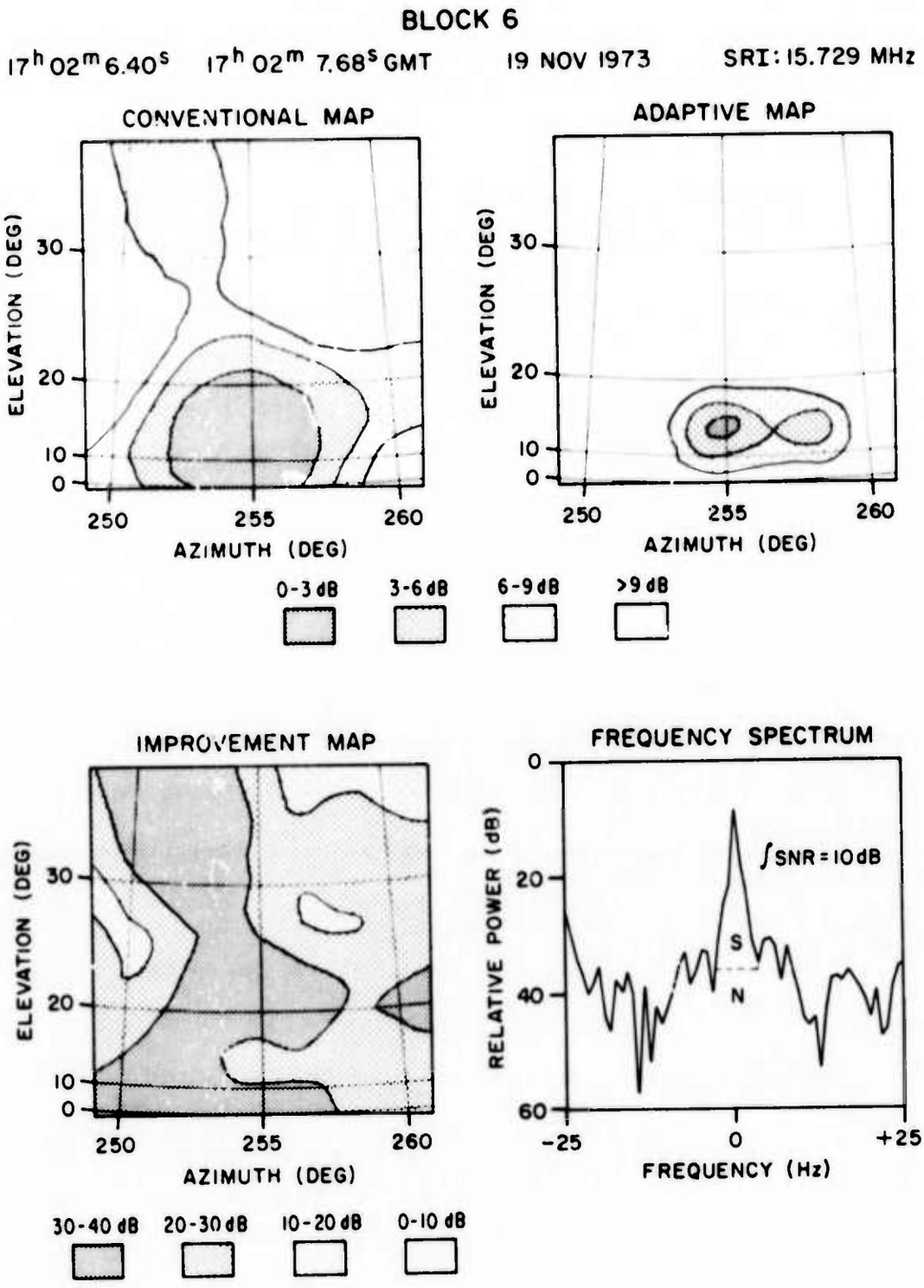

Figure 21. Conventional Map, Adaptive Map, Improvement Map, and Frequency Spectrum for Data Block Number 6.

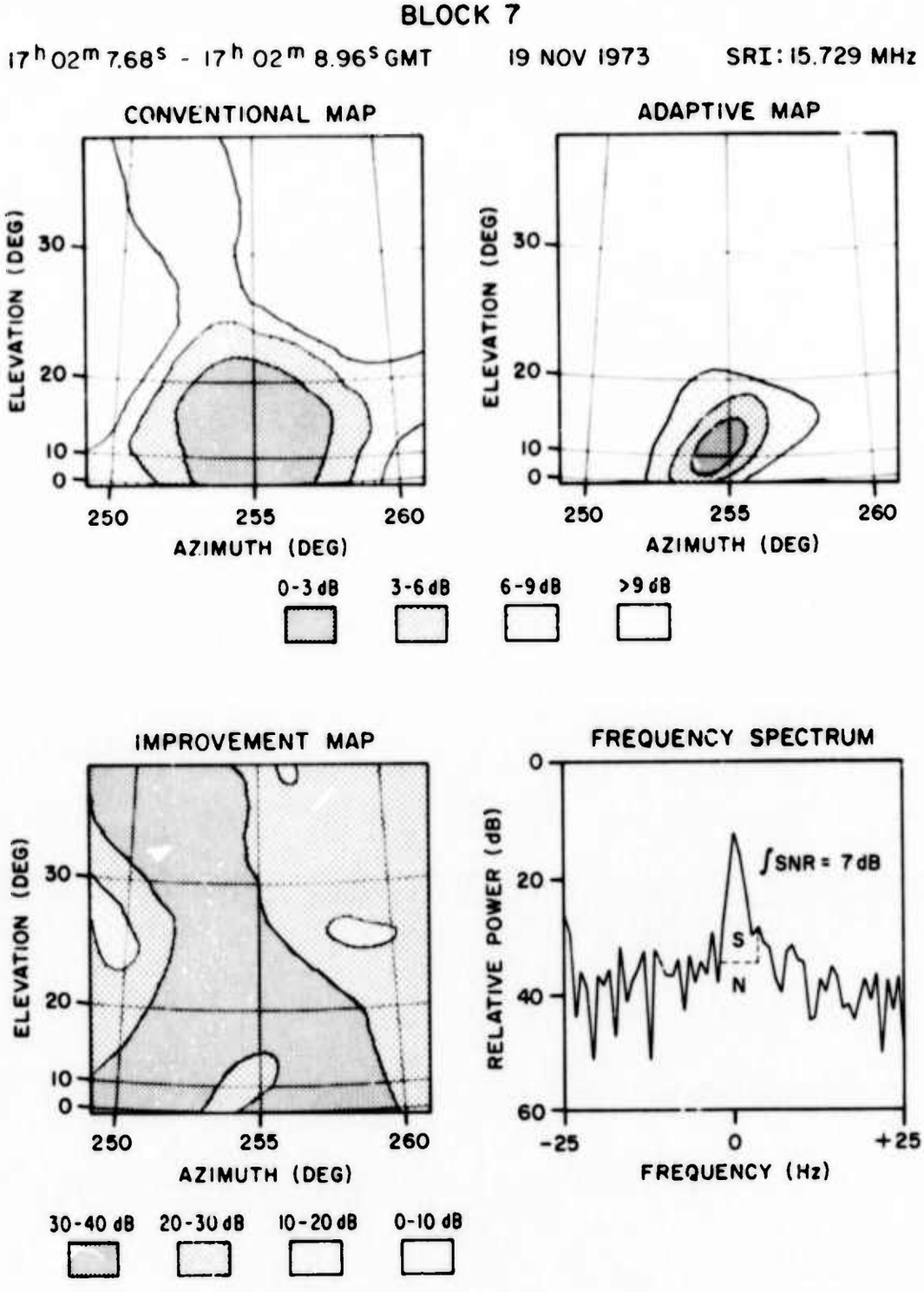

Figure 22. Conventional Map, Adaptive Map, Improvement Map, and Frequency Spectrum for Data Block Number 7.

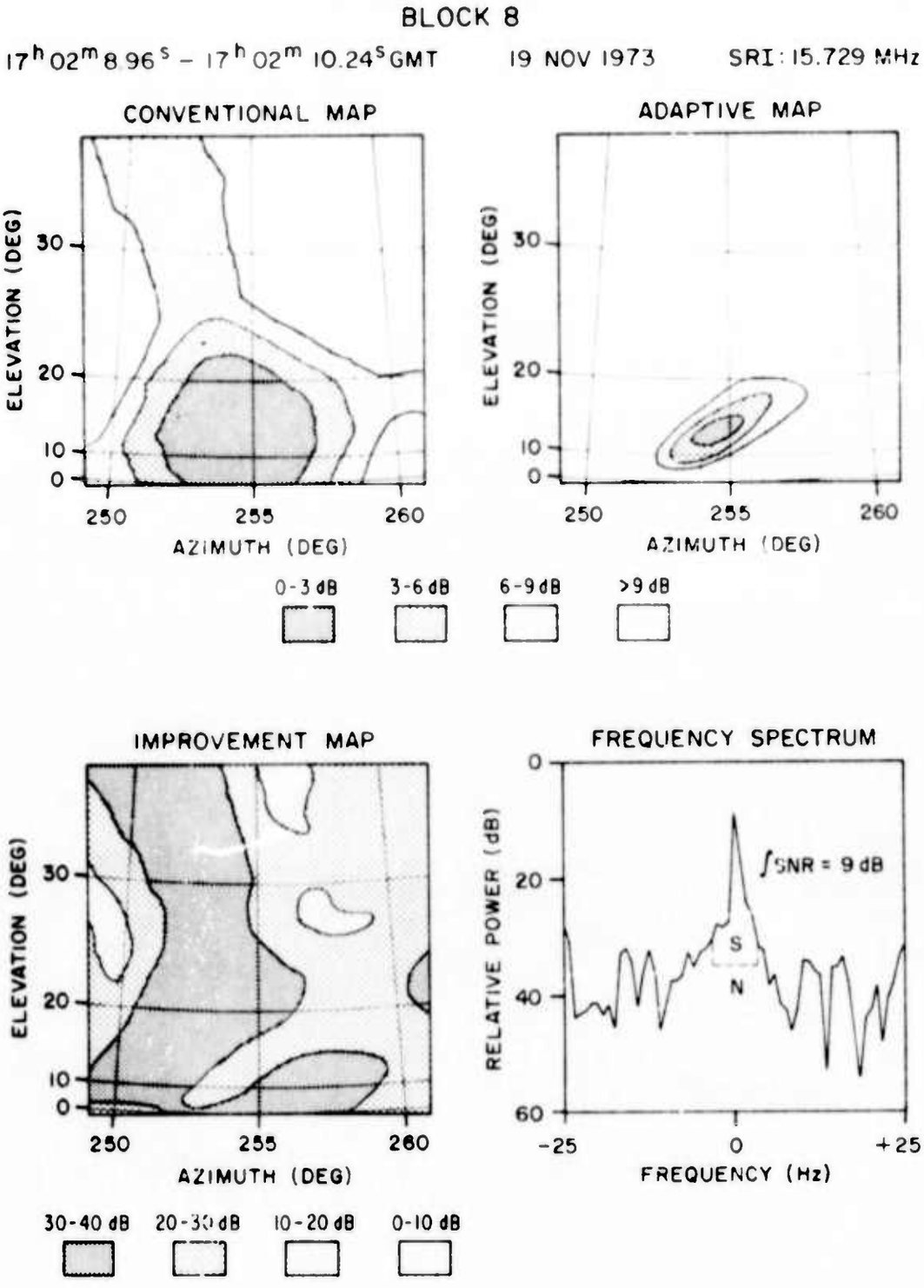

Figure 23. Conventional Map, Adaptive Map, Improvement Map, and Frequency Spectrum for Data Block Number 8.

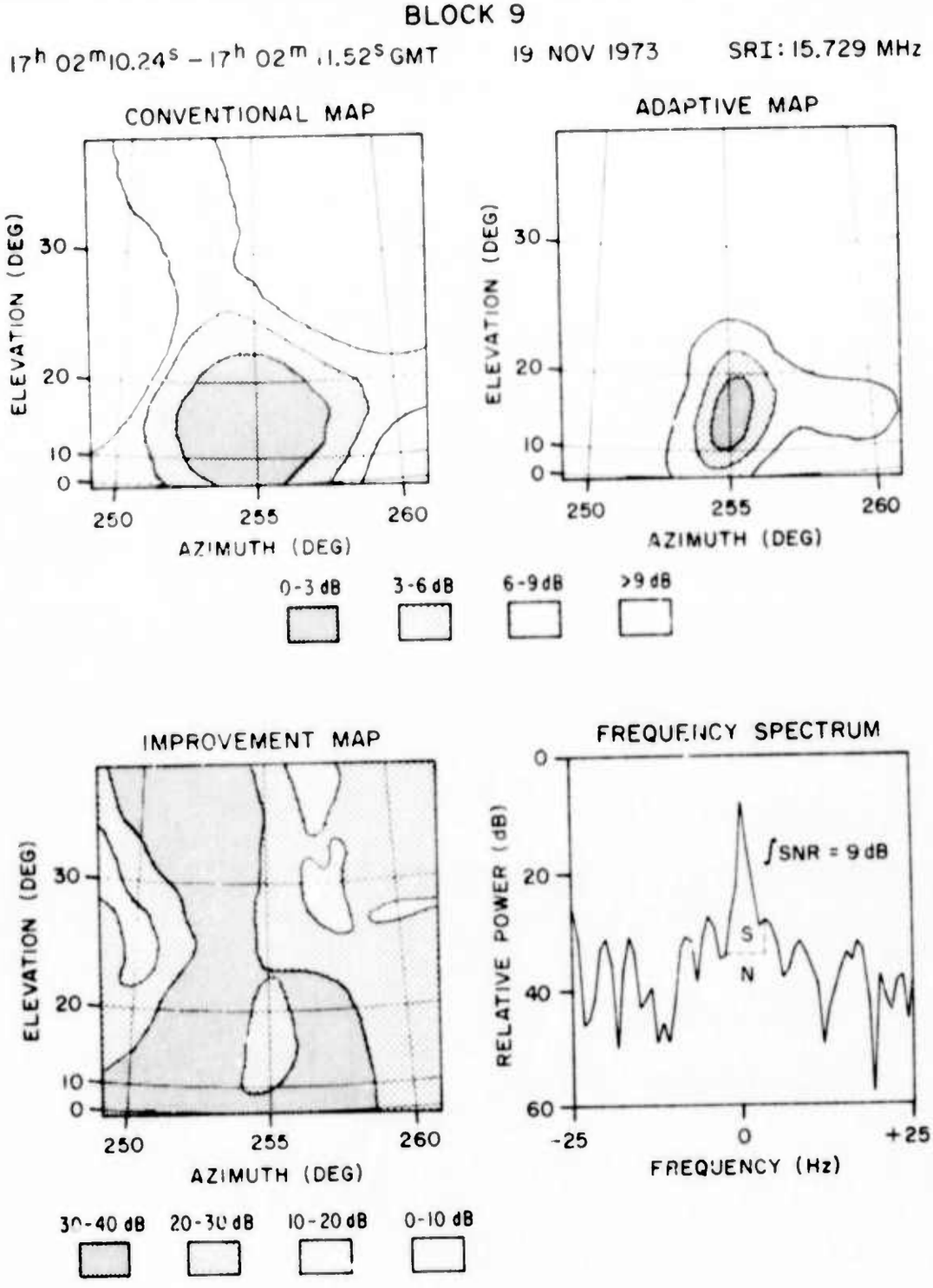

Figure 24. Conventional Map, Adaptive Map, Improvement Map, and Frequency Spectrum for Data Block Number 9.

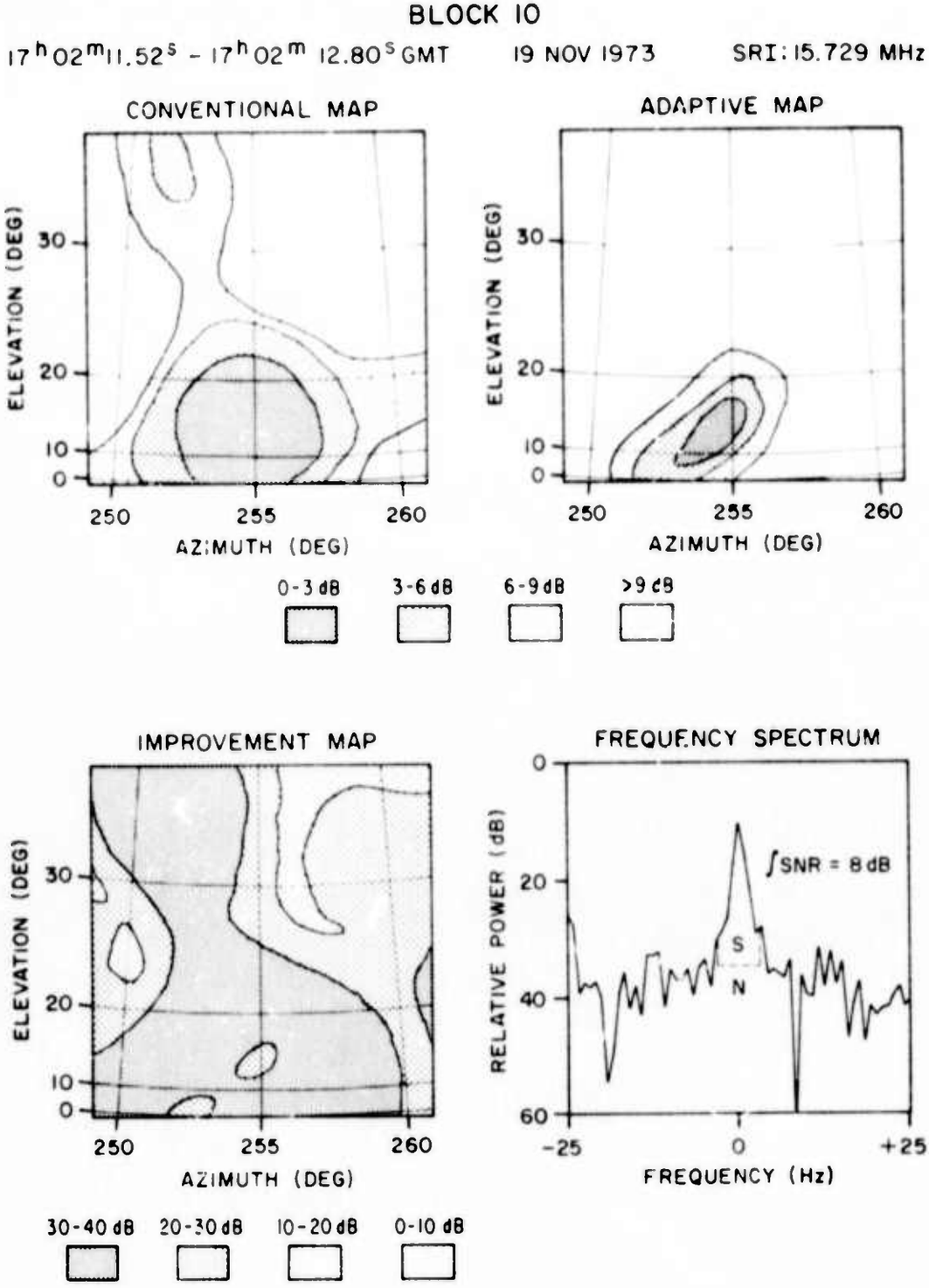

Figure 25. Conventional Map, Adaptive Map, Improvement Map, and Frequency Spectrum for Data Block Number 10.

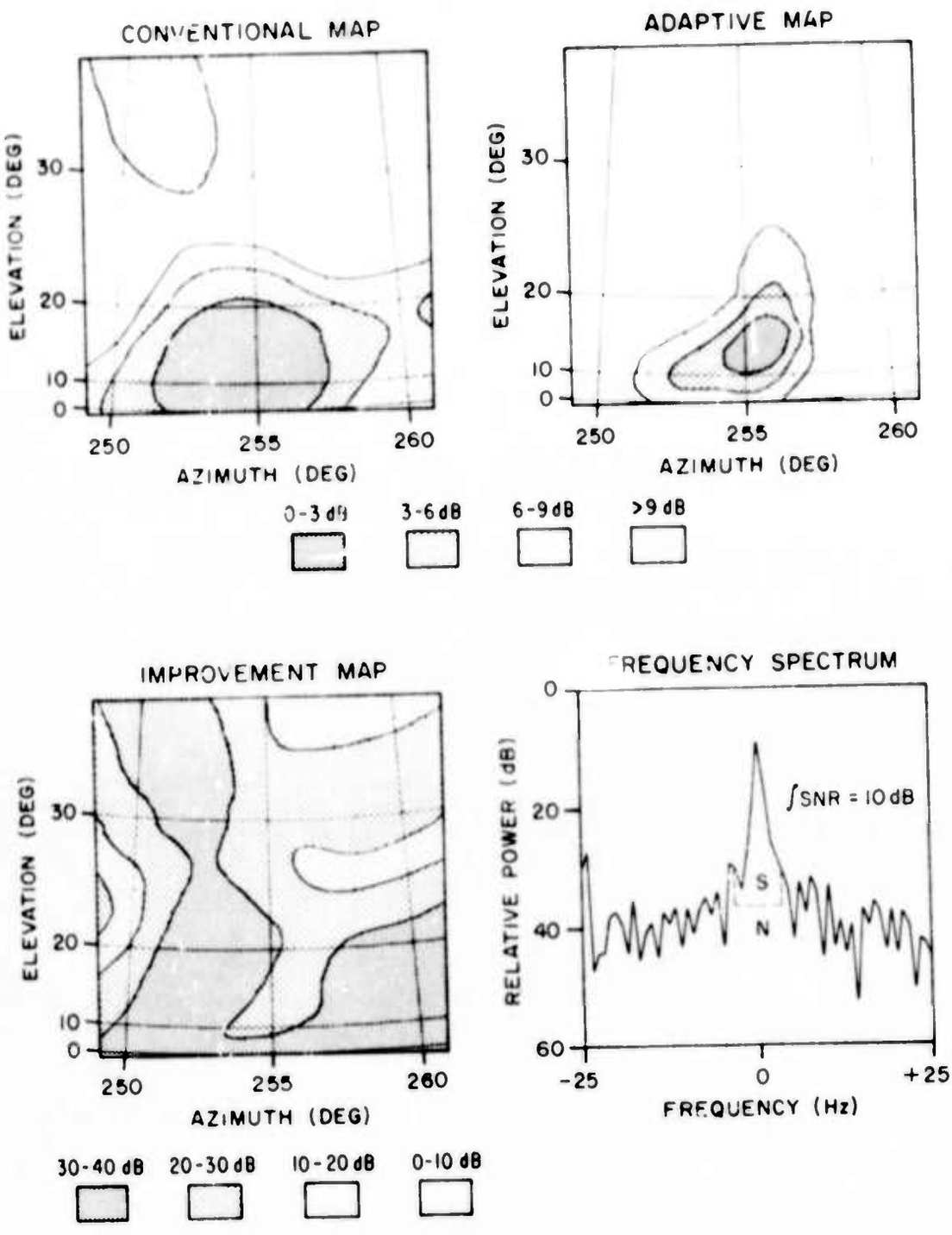

Figure 26. Conventional Map, Adaptive Map, Improvement Map, and Frequency Spectrum for Data Block Number 11.

The one aspect of the results which differ markedly from that expected is the fact that the adaptive processor output is consistenly well below (of order 20 dB) the output of the conventional processor when both are steered in the direction of the interferer, an effect tentatively attributed to the finite angular extent of the incident signal, and the greater sensitivity of adaptive processors to such departures than of conventional processors.

The last topic to be discussed in this section is the stability of the medium, as it affects the noise floor reduction achieved through adaptive processing. The cost of implementing an adaptive processor in real time depends, among other things, upon how frequently one must update the adaptive weights. The improvement maps shown to this point were computed with weights optimized for each data block. If instead, the data for each block were analyzed with the weights computed for the preceding block, the noise floor reduction would be less: the question is "how much less?". Figures 27 through 36 compare the improvement maps obtained using current weights (left) and using weights 1 block old (right). The results vary somewhat from block to block and from one position in the map to another but in round numbers there is a 10 dB loss in improvement if weights for the preceeding 1 second data block are used. By way of comparison, Griffiths (reference 6) found using 8 second data blocks that the penalty paid for using weights optimizedfor the preceding block was also of order of 10 dB. It must be cautioned that the experimental conditions were quite different in these two sets of measurements and that the data base in both cases was very limited. However, it appears that shortening the block length from 8 to 1.28 seconds did not reduce the SNR penalty paid for using weights optimized for the preceding block (10 dB). It is clearly important to update the weights for each block but it remains to be seen how the average

BLOCK 2

$17^h\,02^m\,1.28^s - 17^h\,02^m\,2.56^s$ GMT 19 NOV 1973 SRI: 15.729 MHz

IMPROVEMENT MAPS

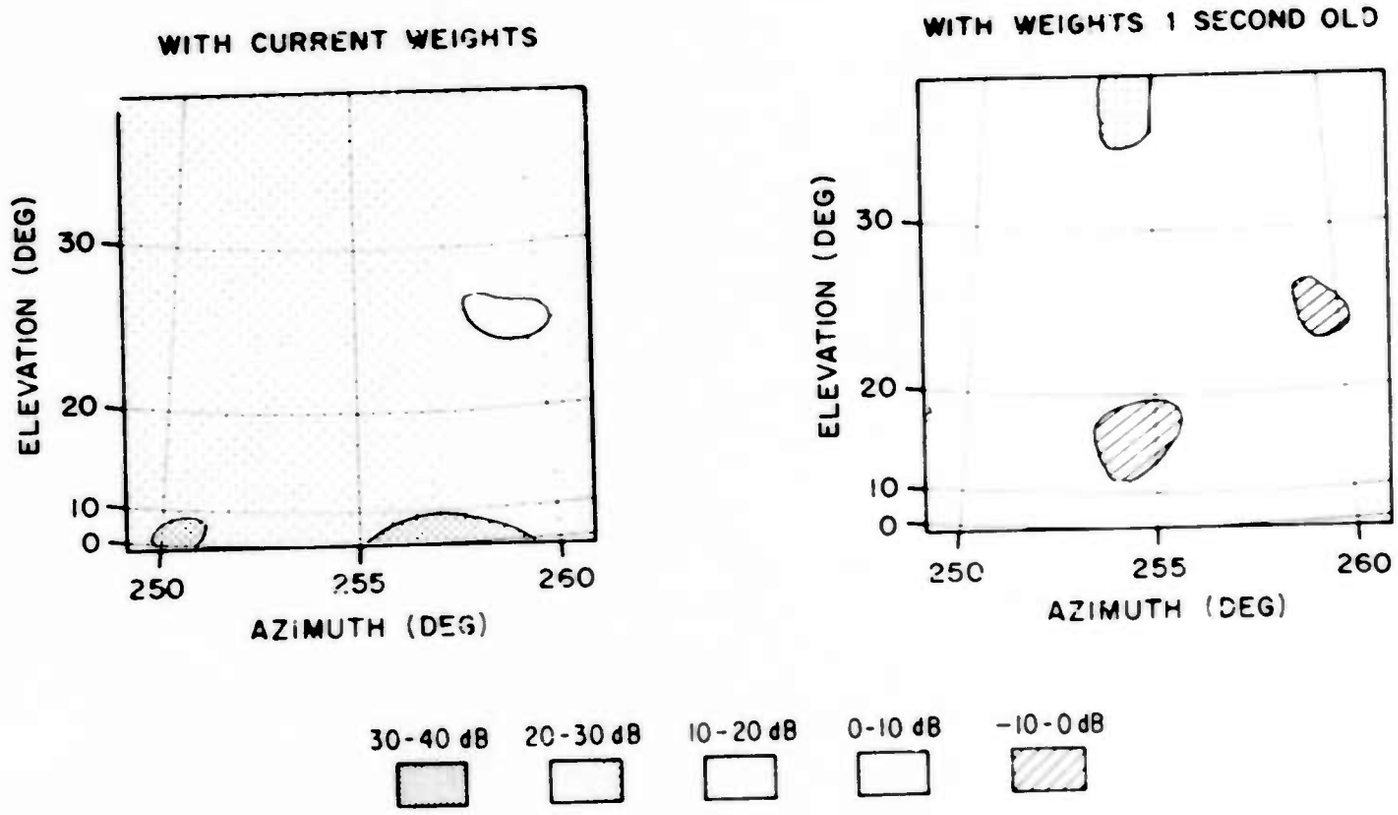

Figure 27. Improvement Maps for Data Block 2 with Optimum Weights (left) and with Weights Optimized for Preceding Block (right).

BLOCK 3

$17^h 02^m 2.56^s - 17^h 02^m 3.84^s$ GMT 19 NOV 1973 SRI: 15.729 MHz

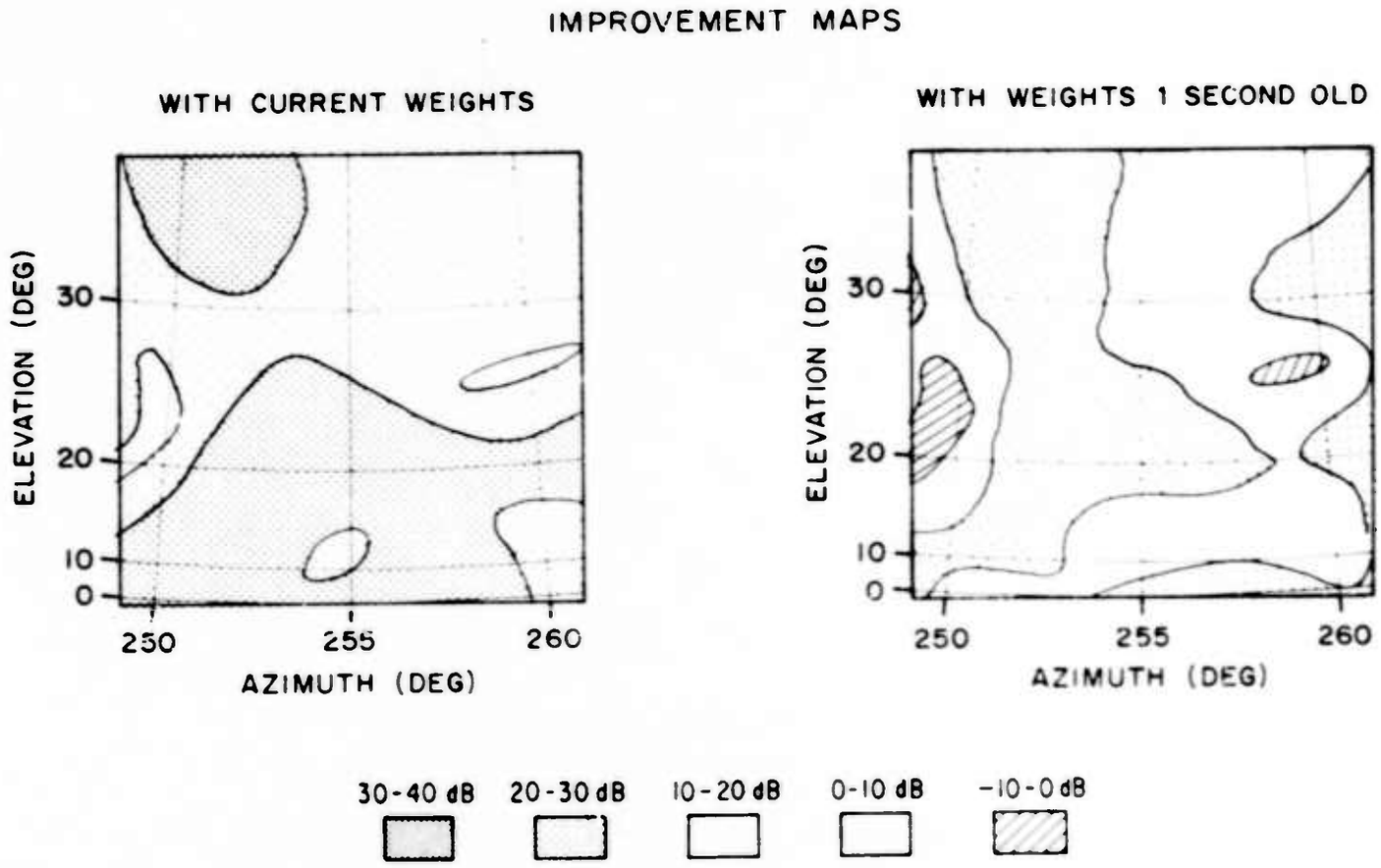

Figure 28. Improvement Maps for Data Block 3 with Optimum Weights (left) and with Weights Optimized for Preceding Block (right).

BLOCK 4

$17^h\,02^m\,3.84^s - 17^h\,02^m\,5.12^s$ GMT 19 NOV 1973 SRI: 15.729 MHz

IMPROVEMENT MAPS

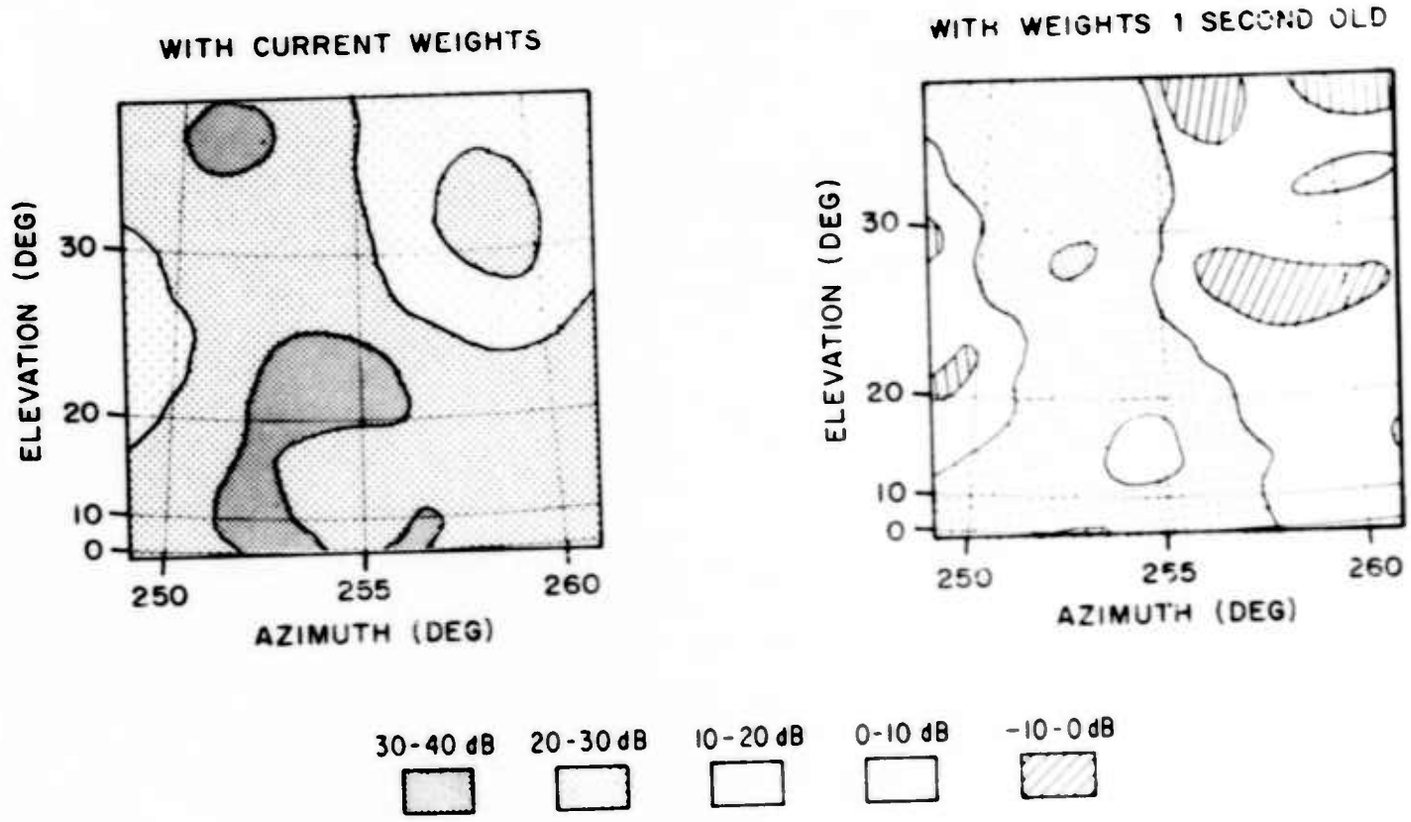

Figure 29. Improvement Maps for Data Block 4 with Optimum Weights (left) and with Weights Optimized for Preceding Block (right).

BLOCK 5

$17^h 02^m 5.12^s - 17^h 02^m 6.40^s$ GMT 19 NOV 1973 SRI: 15.729 MHz

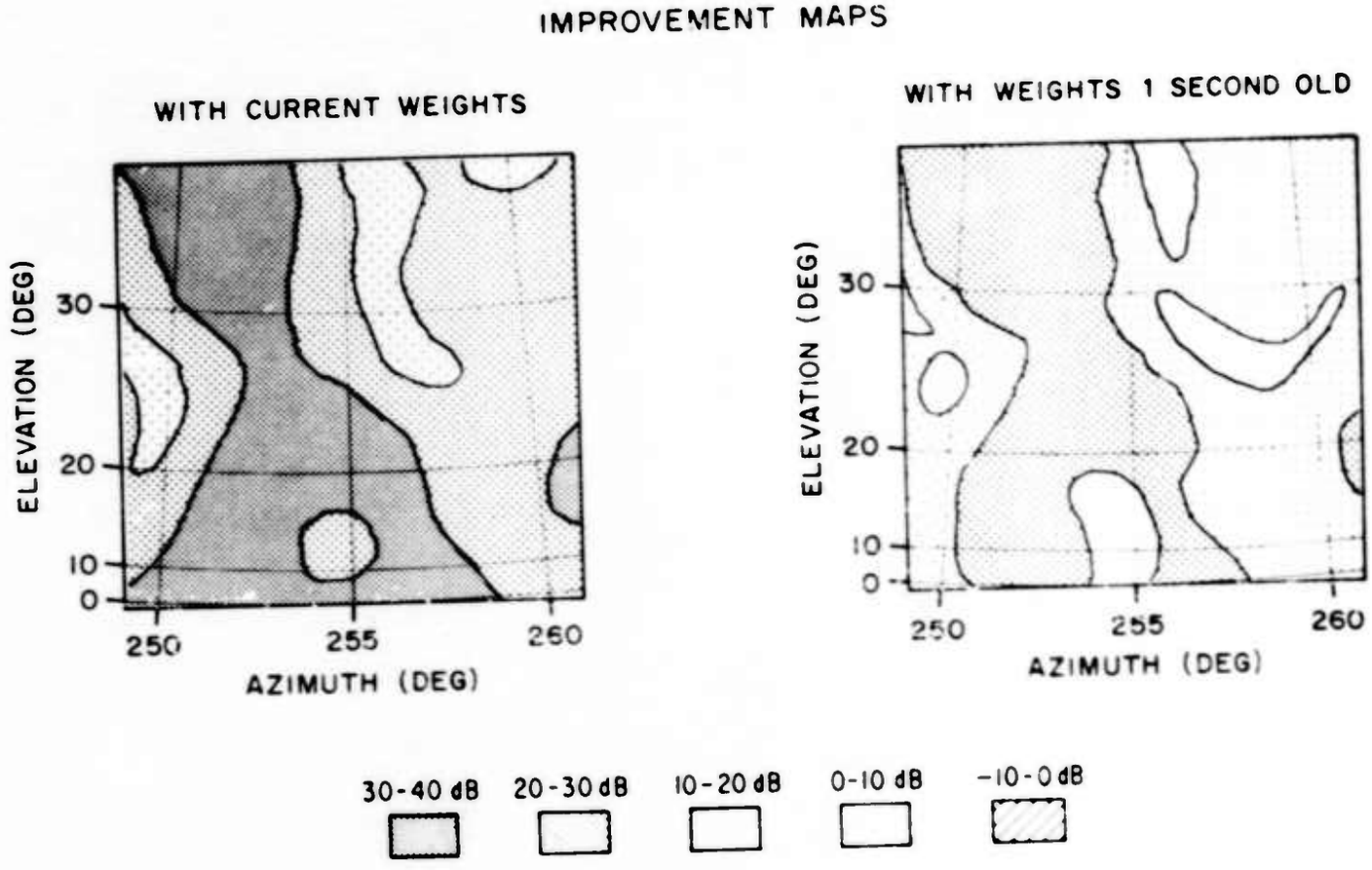

Figure 30. Improvement Maps for Data Block 5 with Optimum Weights (left) and with Weights Optimized for Preceding Block (right).

BLOCK 6

$17^h 02^m 6.40^s$ $17^h 02^m 7.68^s$ GMT 19 NOV 1973 SRI: 15.729 MHz

IMPROVEMENT MAPS

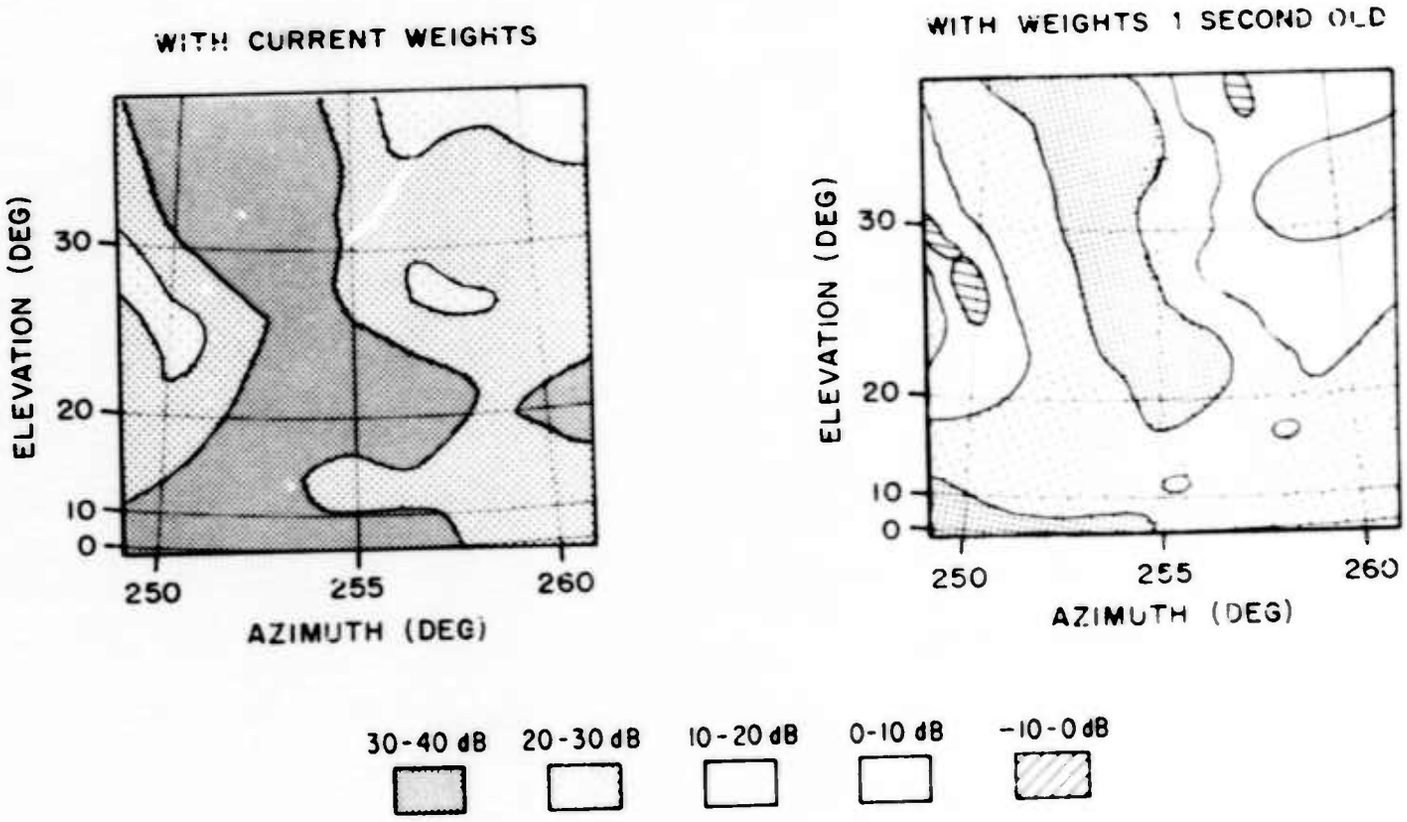

Figure 31. Improvement Maps for Data Block 6 with Optimum Weights (left) and with Weights Optimized for Preceding Block (right).

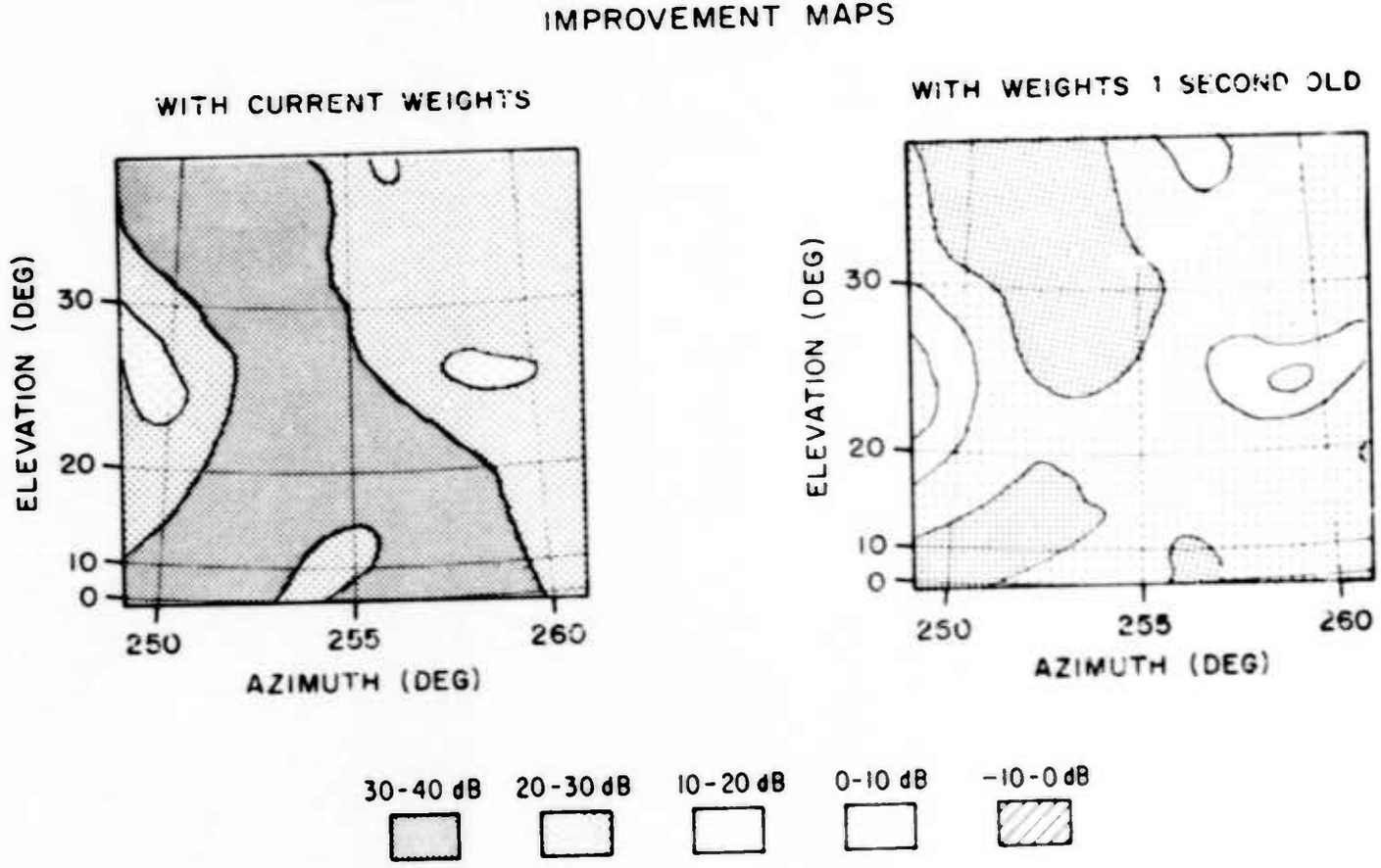

Figure 32. Improvement Maps for Data Block 7 with Optimum Weights (left) and with Weights Optimized for Preceding Block (right).

BLOCK 8

$17^h 02^m 8.96^s - 17^h 02^m 10.24^s$ GMT 19 NOV 1973 SRI: 15.729 MHz

IMPROVEMENT MAPS

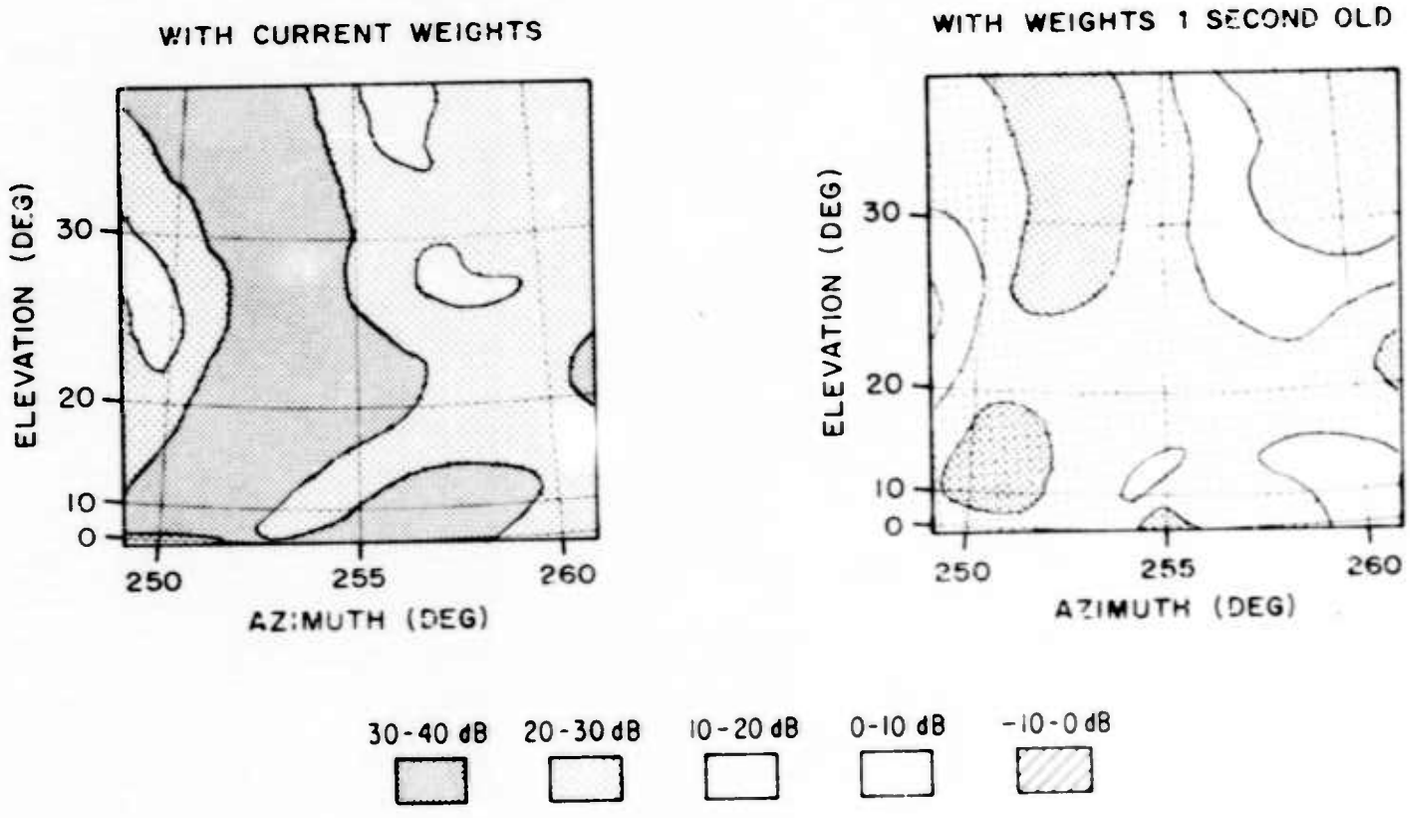

Figure 33. Improvement Maps for Data Block 9 with Optimum Weights (left) and with Weights Optimized for Preceding Block (right).

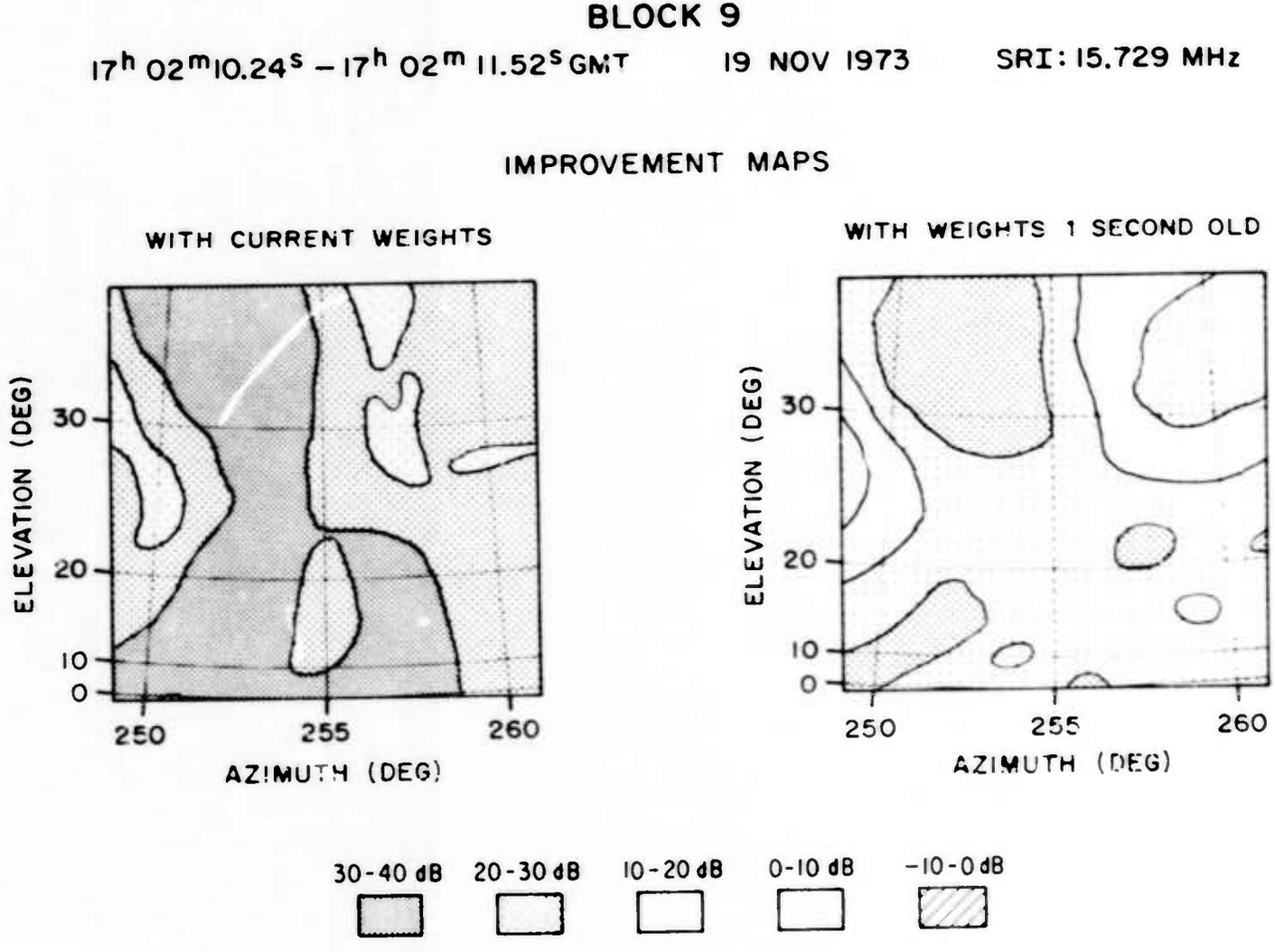

Figure 34. Improvement Maps for Data Block 9 with Optimum Weights (left) and with Weights Optimized for Preceding Block (right).

BLOCK 10

$17^h02^m11.52^s - 17^h02^m 12.80^s$ GMT 19 NOV 1973 SRI: 15.729 MHz

IMPROVEMENT MAPS

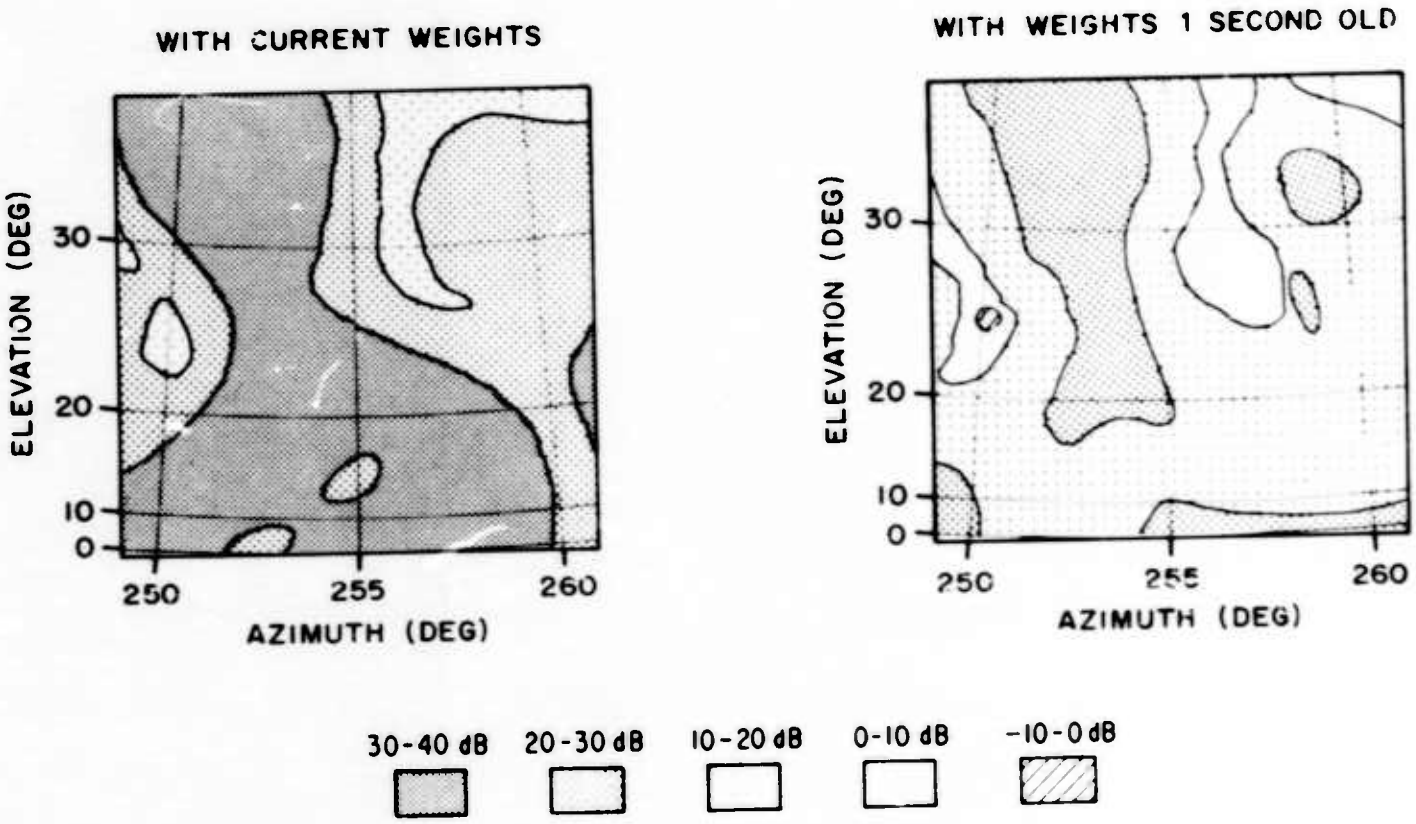

Figure 35. Improvement Maps for Data Block 10 with Optimum Weights (left) and with Weights Optimized for Preceding Block (right).

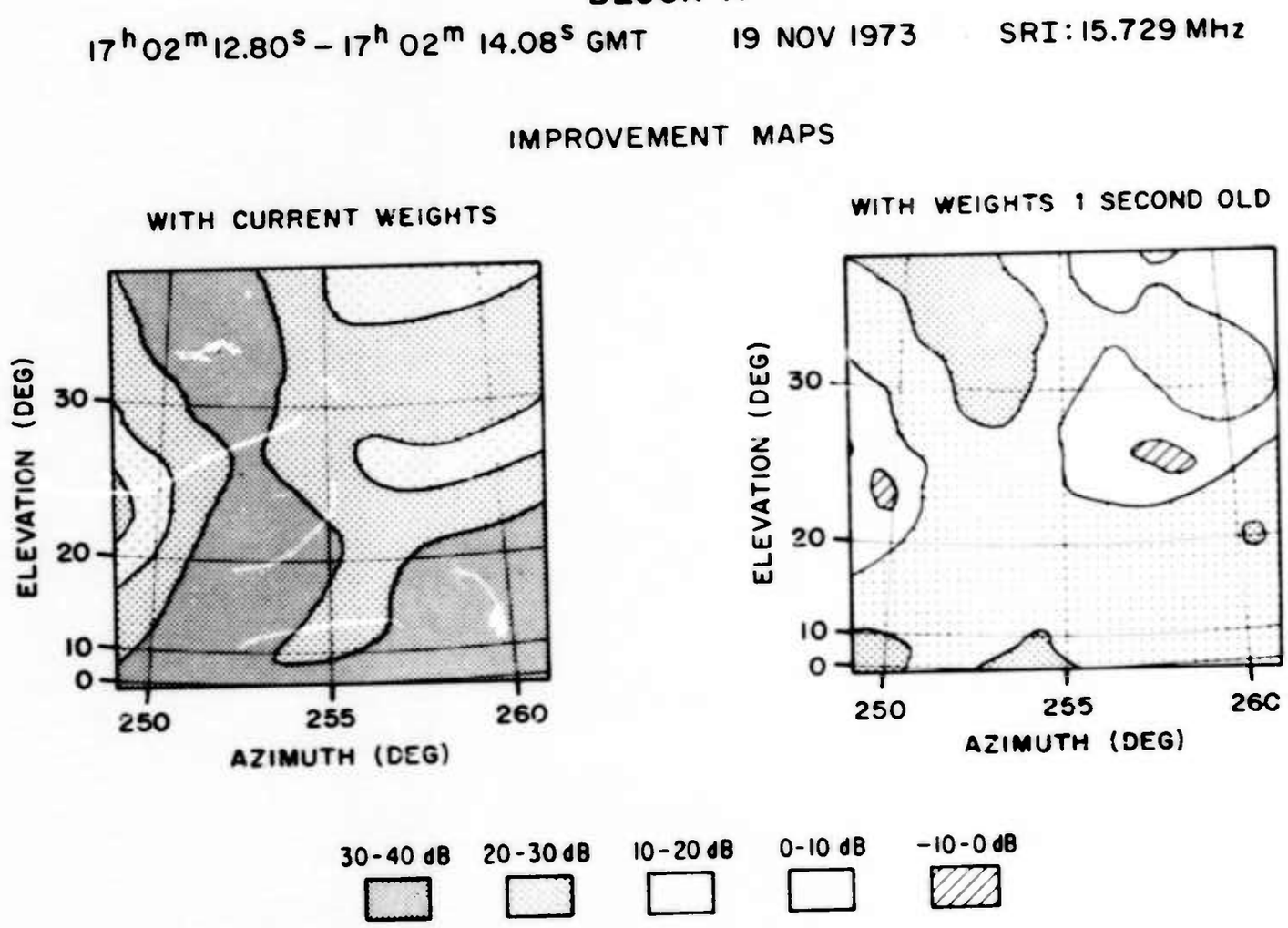

Figure 36. Improvement Maps for Data Block 11 with Optimum Weights (left) and with Weights Optimized for Preceding Block (right).

SNR for a block depends upon block length. The processing load will decrease as the block length increases (the time consuming operation is the matrix inversion required once per block to update the weights). The data on tape should be reprocessed with progressively longer block lengths to see how the SNR improvement varies with block length.

There are several other areas of the analysis which remain unexplored. The data presented in this section should be reprocessed after first filtering in the frequency domain to improve the SNR (the improvement expected is about 16 dB). OTH radar systems will have to do this to achieve target detectability and it is of interest to see what happens to the improvement stability times as the bandwidth becomes less than the signal bandwidth. Increased SNR will also permit us to make a more stringent test of the nulling capability of a practical two-dimensional array, in that sidelobe responses are now undetectable in the adapted maps.

The data taken with both 1 and 2 hop signals from SRI presented simultaneously should be analyzed to examine the performance of an adaptive processor under the common situation in which a strong interferer arrives via two or more modes well separated in elevation angle. The two-hop signal could be viewed as a desired signal and the one-hop as the interferer, for example: a two-dimensional array should be able to deal with this situation effectively whereas a one-dimensional array (azimuth only) could not.

Finally, the data taken under conditions of heavy, multiple source interference (Ham bands, international broadcast bands) should be used to examine the processor performance under conditions where the number of sources are greater than the number of array elements (which determines the number of degrees of freedom available and the number of nulls which can be steered).

6.0 SUMMARY AND CONCLUSIONS

The DARPA phased array facility near Hudson, Colorado has been modified to permit the collection of a data base on a two-dimensional HF array in a format suitable for adaptive processing. This has included the fabrication and installation of 32 receivers, 32 vertical monopole elements with base amplifiers, and the development of software for controlling the data acquisition and recording system. Data have been collected under a variety of conditions and in a form such that adaptive processing can be done in azimuth, in elevation, in frequency, or in any combination of these. Analysis software has been written to reduce the data with conventional beamforming algorithms and with existing adaptive beamforming algorithms (direct matrix inversion). Analysis software has also been written to produce simulated data tapes for model environments and model array configurations: these have been used to verify the data reduction software and to study the effect of array configuration on adaptive antenna performance. The field data tapes have been made available to the DARPA community and a limited amount of analysis of these tapes has been done at Raytheon. The principal findings of this analysis are the following:

1. Verification that the HF environment will in fact permit several of the benefits anticipated from numerical simulations; notably,
   a. Noise Floor Reduction: reduction of the noise floor by 30 dB or more over much of the sky. This was achieved with pattern control alone (adapting in azimuth and elevation but not in frequency) against an interferer of modest

strength (10 dB SNR measured at the element).

b. Sidelobe Reduction: an alternate way of viewing the noise floor reduction achieved is that the effective sidelobe levels of the antenna were reduced by more than 30 dB. For the data examined to date (a single dominant interferer with SNR of 10 dB at the element) the effect of antenna sidelobes were not merely reduced but were eliminated, in that sidelobe responses were undetectable in the adaptively processed data.

c. Effective Beamwidth: the effective 3 dB beamwidth of the antenna array (after processing) was reduced by as much as a factor of 6 when used to map isolated signals having element SNR's of order 10 dB. That is, the apparent angular width of discrete sources on sky maps was much narrower with adaptive processing than with conventional processing.

2. Measurement of the following properties of the environment which impact directly on the usefulness of adaptive processing at HF:

a. Stability of the Environment: the environment changes rapidly enough so that if the optimum adaptive weights are replaced by weights 1 second old, the loss in noise floor reduction is order 10 dB. For a situation in which the noise floor reduction with optimum weights was 30 dB, this means that the reduction will be only of order 20 dB if weights 1 second old are used. The upshot of this is to suggest that in practice the adaptive weights will have to be recomputed for each data block: it remains to be seen how long individual data blocks can be without significant SNR penalty.

b. Limitations of Plane-Wave Idealization: For an ideal antenna (identical element patterns, no calibration errors), ideal terrain (no scattering from local structures), and ideal ionospheric reflection (single discrete mode), the amplitude of the signal would be uniform across the array and the phase would vary linearly. For this case the output of conventional and adaptive processors would be the same when steered to the source direction. In practice, however, it was found that the departures from ideal were enough (e.g., RMS amplitude variations of a few tens of percent across the array) to cause the output of the adaptive processor to be 20 to 30 dB less than the output of the conventional processor when steered in the source direction. This result was unexpected, though in retrospect it could have been predicted from the RMS variation from plane wave conditions reported for other large HF arrays and numerical simulations of the impact of such variations on adaptive processor performance. It is not known to what extent the observed departure from the plane wave idealization is due to residual system calibration errors, scattered fields from local irregularities, or irregularities introduced by the ionospheric reflection process. The recommendation is that future data collection efforts be preceded by a test in which a beacon transmitter is flown across the array to verify the calibration of the system as a whole (antenna and local terrain). It should be emphasized that the impact of departures from ideal plane wave conditions depends upon the SNR of the discrete signal and may not be a problem

for the low SNR signals of common interest in applications.

3. The effect of array configuration on adaptive processor performance was considered from the viewpoint of the system designer seeking to place the available elements to best advantage: low redundancy sparse arrays (be they one or two dimensional) are suggested as promising configurations for making the most of the elements and processing capability available. It has not been shown rigorously that such arrays are "best" in any specific sense but numerical simulations and comparisons with field data make it plausible for situations in which the goal is not merely to detect a signal (maximize SNR) but also to tell where it's coming from (maximize angular resolution).

7.0 REFERENCES

1. Thome, G. D. and R. L. St. Germain, Evaluation of Two Dimensional Adaptive Antenna Arrays, Raytheon Company, RADC-TR-74-186, 1974.

2. Griffiths, L. J., A simple Adaptive Algorithm for Real-Time Processing in Antenna Arrays, Proc. IEEE, Vol. 57, No. 10, 1969.

3. Capon, J., High-Resolution Frequency-Wave number Spectrum Analysis, Proc. IEEE, Vol. 57, No. 8, 1969.

4. McDonough, R. N., Degraded Performance of Nonlinear Array Processors in the Presence of Data Modeling Errors, J. Acoust. Soc. Am., Vol. 51, 1973.

5. Moffet, A. T., Minimum Redundancy Linear Arrays, IEEE Transactions on Antennas and Propagation, Vol. AP-16, No. 2, 1968.

6. Griffiths, L. J., Adaptive Array Processing of HF Signals Propagated Over a 2600 km Path, University of Colorado, RADC-TR-73-75, 1973.

MISSION
of
Rome Air Development Center

RADC is the principal AFSC organization charged with planning and executing the USAF exploratory and advanced development programs for electromagnetic intelligence techniques, reliability and compatibility techniques for electronic systems, electromagnetic transmission and reception, ground based surveillance, ground communications, information displays and information processing. This Center provides technical or management assistance in support of studies, analyses, development planning activities, acquisition, test, evaluation, modification, and operation of aerospace systems and related equipment.

Source AFSCR 23-50, 11 May 70